7-2020

DEVELOPING A NEW FORMULA FOR PREDICTING OIL RECOVERY FACTOR IN WATER FLOODED-HETEROGENEOUS RESERVOIRS

Mohamed Khaled Aljifri

United Arab Emirates University

College of Engineering

Department of Chemical and Petroleum Engineering

DEVELOPING A NEW FORMULA FOR PREDICTING OIL RECOVERY FACTOR IN WATER FLOODED-HETEROGENEOUS RESERVOIRS

Mohamed Khaled Aljifri

This thesis is submitted in partial fulfilment of the requirements for the degree of Master of Science in Petroleum Engineering

Under the Supervision of Dr. Hazim Al-Attar

July 2020

Declaration of Original Work

I, Mohamed Khaled Aljifri, the undersigned, a graduate student at the United Arab Emirates University (UAEU), and the author of this thesis entitled *"Developing a new Formula for Predicting Oil Recovery Factor in Water Flooded-heterogeneous Reservoirs",* hereby, solemnly declare that this thesis is my own original research work that has been done and prepared by me under the supervision of Dr. Hazim Al-Attar, in the College of Engineering at UAEU. This work has not previously been presented or published, or formed the basis for the award of any academic degree, diploma or a similar title at this or any other university. Any materials borrowed from other sources (whether published or unpublished) and relied upon or included in my thesis have been properly cited and acknowledged in accordance with appropriate academic conventions. I further declare that there is no potential conflict of interest with respect to the research, data collection, authorship, presentation and/or publication of this thesis.

Student's Signature:  Date: 9/7/2020

Approval of the Master Thesis

This Master Thesis is approved by the following Examining Committee Members:

1) Advisor (Committee Chair): Hazim Al-Attar
   Title: Associate Professor
   Department of Chemical and Petroleum Engineering
   College of Engineering

   Signature 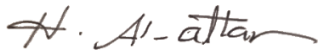 Date: 16/07/2020

2) Member: Abdul Razzag Bin Zekri
   Title: Professor
   Department of Chemical and Petroleum Engineering
   College of Engineering

   Signature  Date: 16/07/2020

3) Member: Quoc Nguyen
   Title: Professor
   Hildebrand Department of Petroleum and Geosystems Engineering
   Institution: University of Texas at Austin, USA

   Signature 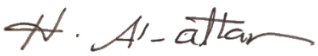 Date: 16/07/2020

This Master Thesis is accepted by:

Dean of the College of Engineering: Professor Sabah Al-Kass

Signature  Date 12/10/2020

Dean of the College of Graduate Studies: Professor Ali Al-Marzouqi

Signature  Date 12/10/2020

Copy ____ of ____

Abstract

In this work, two sets of empirical correlations were developed for predicting the recovery factor (RF) in water-flooded layered oil reservoirs. The first set of these correlations encompasses four key parameters believed to have significant impact on water flooding performance, namely, reservoir heterogeneity (permeability variation coefficient), injected water viscosity, permeability anisotropy (ratio of vertical permeability to horizontal permeability), and water injection rate. This first set consists of two expanded forms, one for predicting the RF at water breakthrough time (BT) and the other for predicting the RF at the end of project (EOP). Out of the aforementioned four key parameters, the second set of the developed correlations only considers the parameters that have been found most effective in the process of water flooding. Thus, the second set consists of two reduced forms, one for predicting the RF at BT (RF_{BT}) and the other for predicting the RF at EOP (RF_{EOP}).

In the development process of the new correlations, the ECLIPSE simulator was used to generate a large number of data points representing, among other profiles, the RF and water cut performances for various combination scenarios of the above key parameters. These simulation-generated data were then processed by the General Linear Model analysis technique to develop the target empirical correlations.

When tested against 144 simulation-generated data points used in their development, the expanded forms of the new correlations have been found to give reliable estimates of RF_{BT} and RF_{EOP} with AAPCD of 6.9 and 1.02, respectively. The reduced forms were found to yield a slightly higher AAPCD for the same data set. When tested against 48 simulation-generated data points not included in the development of the proposed correlations, the expanded forms of the new correlations have been found to give good estimates of RF_{BT} and RF_{EOP} with AAPCD of 6.5 and 14, respectively. The new correlations have been found to give more accurate estimates of RF_{EOP} than for RF_{BT}. The highest RF_{EOP} of 50.6% was achieved for a combination scenario defined by: q_i = 10,000 bpd, μ_w = 1.0 cp, k_z/k_x = 1.0, and V = 0.1. When tested against two published empirical correlations using a single

field data point, the proposed correlations were found to give relatively high APCD but still comparable to the API method.

Keywords: Reservoir heterogeneity, Injected water rate, Permeability anisotropy, Water viscosity, General linear model.

Title and Abstract (in Arabic)

تطوير صيغة جديدة للتنبؤ بعامل استخلاص الزيوت في الخزانات التي تغمرها المياه

الملخص

في هذا العمل، تم تطوير مجموعتين من الارتباطات التجريبية للتنبؤ بعامل الاسترداد في خزانات النفط ذات الطبقات المغمورة بالمياه. تشمل المجموعة الأولى من هذه الارتباطات أربعة معلمات رئيسية يعتقد أنها لها تأثير كبير على أداء فيضان المياه، وهي عدم تجانس الخزان (معامل تغير النفاذية)، لزوجة الماء المحقونة، تباين النفاذية (نسبة النفاذية الرأسية إلى النفاذية الأفقية)، ومعدل حقن الماء. تتكون هذه المجموعة الأولى من شكلين موسعين، أحدهما للتنبؤ بعامل الاسترداد في وقت اختراق المياه والآخر للتنبؤ بعامل الاسترداد في نهاية المشروع. من بين المعلمات الرئيسية الأربعة المذكورة أعلاه، فإن المجموعة الثانية من الارتباطات المطورة تأخذ في الاعتبار فقط المعلمات التي تم العثور عليها الأكثر فعالية في عملية غمر المياه. وهكذا، تتكون المجموعة الثانية من شكلين مخفضين، أحدهما للتنبؤ بعامل الاسترداد عند في وقت احتراق الماء والآخر للتنبؤ بعامل الاسترداد في نهاية المشروع.

في عملية تطوير الارتباطات الجديدة، تم استخدام جهاز محاكاة (ECLIPSE) لتوليد عدد كبير من نقاط البيانات التي تمثل، من بين ملفات التعريف الأخرى، أداء عامل الاسترداد وقطع المياه لمختلف سيناريوهات الجمع للمعلمات الرئيسية المذكورة أعلاه. ثم تمت معالجة هذه البيانات الناتجة عن المحاكاة بواسطة تقنية تحليل النموذج الخطي العام لتطوير الارتباطات التجريبية المستهدفة.

عند اختبارها مقابل 144 نقطة بيانات تم إنشاؤها في المحاكاة والمستخدمة في تطويرها، تم العثور على الأشكال الموسعة للارتباطات الجديدة لإعطاء تقديرات موثوقة لـ عامل الاسترداد في وقت اختراق المياه ونهاية المشروع مع متوسط فرق النسبة المطلقة من 6.9 و 1.02، على التوالي. تم العثور على النماذج المصغرة لإعطاء متوسط فرق النسبة المطلقة أعلى قليلاً لمجموعة البيانات نفسها. عند اختبارها مقابل 48 نقطة بيانات تم إنشاؤها في المحاكاة غير مدرجة في تطوير الارتباطات المقترحة ، تم العثور على الأشكال الموسعة للارتباطات الجديدة لإعطاء تقديرات جيدة لـعامل الاسترداد في وقت اختراق المياه ونهاية المشروع مع متوسط فرق النسبة المطلقة من 6.5 و 14،

على التوالي. تم العثور على الارتباطات الجديدة لإعطاء تقديرات أكثر دقة لـعامل الاسترداد في وقت اختراق المياه عن نهاية المشروع. تم تحقيق أعلى عامل استرداد في نهاية المشروع بنسبة 50.6٪ لسيناريو الجمع المحدد بواسطة: معدل حقن الماء = 10000 برميل في اليوم، لزوجة الماء = 1.0 ، تباين النفاذية = 1.0، وعامل عدم تجانس الخزان =0.1. عند اختبارها مقابل ارتباطين تجريبيين منشورين باستخدام نقطة بيانات حقل واحدة، تم العثور على الارتباطات المقترحة لإعطاء فرق النسبة المطلقة عالية نسبيًا ولكن لا تزال قابلة للمقارنة مع طريقة (API).

مفاهيم البحث الرئيسية: عدم تجانس الخزان، معدل حقت الماء، تباين النفاذية، لزوجة الماء المحقونة، تقنية تحليل النموذج الخطي العام.

Acknowledgements

My thanks go to Dr. Hazim Al-Attar whose enthusiasm about and introduction to my project and his great knowledge in the theory got me started and whose endless ideas and encouragement led to this and most other studies in which I have been involved. I am especially grateful to Dr. Fathi Boukadi who helped with Eclipse Software and solved the issues that I faced and guided me throughout this project.

I would like to thank the chair and all members of the Department of Chemical and Petroleum Engineering at the United Arab Emirates University for assisting me all over my studies and research. Special thanks go to my parents, brother, and sister who helped me along the way. I am sure they suspected it was endless.

Dedication

To my beloved parents and family

Table of Contents

List of Tables

List of Figures

List of Abbreviations

A	Area, acres
Bo	Oil Formation Volume Factor, rb/stb
h	Thickness, ft
k	Permeability, md
M	Mobility Ratio
P	Pressure, psia
q_i	Water Injection Rate, stb/d
V	Permeability Variation Coefficient
ϕ	Porosity
BT	Breakthrough
ECL	Exploration Consultants Limited
ECM	Empirical Correlation Method
EOP	End of Project
RF	Recovery Factor
RF_{BT}	Recovery Factor at Breakthrough
RF_{EOP}	Recovery Factor at End of Project
μ_o	Oil Viscosity, cP
μ_w	Water Viscosity, cP
k_{ro}	Relative Permeability to Oil
k_{rw}	Relative Permeability to Water
k_z/k_x	Permeability Anisotropy Ratio

S_w	Water Saturation

Chapter 1: Introduction

1.1 Water flooding

Water flooding has been the fundamental method of secondary oil recovery since 1865. The oil industry has adopted this method because of abundance of water supply, which renders the process to be inexpensive. In addition to its stability as a drive mechanism, water flooding accomplishes two purposes in maintaining the reservoir pressure and pushing the oil towards the producers. Consequently, accurate prediction of water flooding performance plays a crucial role in achieving better overall reservoir management and better overall project economics.

Water flooding in heterogeneous reservoir sections (weather 3D or 2D) is far more complex than the one-dimensional laboratory water flooding in small core samples. The efficiency of the process in hillsides is controlled by three physical factors: (1) mobility ratio, (2) heterogeneity, and (3) gravity. Accordingly, various analytical models and numerical reservoir simulators were developed to facilitate the prediction of water flooding performance with high accuracy. Depending on the experience of the reservoir simulation engineers, however, running industry-standard software packages can be expensive and time consuming. In this study, an easy to apply formula will be developed which can be used to achieve quick and reliable estimates of oil recovery attained by water flooding schemes [1].

There are many field examples for water flooding projects such as the North Sea oil fields. This term refers to areas such as UK, Norway, Netherlands and such more.

These fields have an oil that range from light to heavy oil and applying water flooding have maintained the pressure and increased the oil recovery successfully. Examples of these fields are Ekofisk and Eldfisk oil fields [3].

1.2 Factors to consider in water flooding

In order to determine the suitability of a candidate reservoir for water flooding, it should be taken into consideration the following reservoir characteristics:

1.2.1 Reservoir geometry

It influences the location of the wells and number of platforms. In addition, it will essentially dictate the methods by which a reservoir can be produced through water injection practices [2].

1.2.2 Fluid properties

It has an effect on the suitability of a given reservoir for a further development by water flooding. The viscosity of the crude oil is the most important fluid property that affect the success of a water flooding project. The oil viscosity has the important effect of determining the mobility ratio which controls the sweep efficiency. Lowering the oil viscosity will lead to make the mobility ratio favorable which is most wanted for water flooding projects [2].

1.2.3 Reservoir depth

It has an important influence on both the technical and economic aspects of a secondary or tertiary recovery project. In addition, maximum injection pressure will

increase with depth. Moreover, the cost of lifting oil from very deep wells will limit the maximum economic oil-water ratios that can be tolerated, so that reducing the ultimate recovery factor and increasing the total project operating cost. In water flood projects, there is a critical pressure of approximately 1psi/ft. of depth that if exceeded permits the injection water to expand along fractures or create fracture which results in the channeling of the injected water. Therefore, an operational pressure gradient of 0.75 psi/ft of depth is allowed to provide a sufficient margin of safety to prevent pressure parting [2].

1.2.4 Lithology and pore compaction

It has a profound influence on the efficiency of water injection in a particular reservoir. Reservoir lithology and rock properties that affect flood ability and success are porosity, permeability, clay content and net thickness. In some complex reservoir systems, only a small portion of the total porosity will have sufficient permeability to be effective in water injection operation. Although evidence suggests that clay minerals present in some sands may clog the pores by swelling when water flooding is used, no exact data are available as to the extent to which this may occur. For tight reservoirs, there will be water injection problems in terms of the desired injection rate or pressure.

In general, the high permeability formation (thief zone) will lead rapid channeling and bypassing will develop. Moreover, the lower depletion pressure that may exist in these zones will aggravate the water channeling tendency due to high permeability variation. Therefore, these thief zones will contain less residual oil and their flooding will lead to lower oil recoveries [2].

1.2.5 Rock wettability

It's as the tendency of the fluid to spread on or adhere to a solid surface in the presence of other immiscible fluids. Wettability has a high influence on the oil recovery. The relationship between the wettability and the recovery is being studied since decades. Wettability of a reservoir strongly affects oil recovery efficiency in water flooding projects. In a preferentially water wet system, the oil recovery at breakthrough is high, while water breakthrough occurs earlier at preferentially oil wet system. Water flooding is less efficient in oil wet systems than water wet systems, since a large amount of water is required to recover more oil [2].

1.2.6 Oil volatility

Most of the water drive fields in the North Sea contain oil of moderate to low volatility. The advantage is that gas oil ratios are of a tolerable level making gas disposal fairly straightforward. In addition, these oils are characterized by low oil viscosity which is favorable in water flooding operations.

1.3 The optimum time to water flood

The most common procedure for determining the optimum time to start water flooding depends on the following very important factors:

1.3.1 Reservoir oil viscosity

Water injection should be initiated when the reservoir pressure reaches its bubble point pressure since the oil viscosity reaches its minimum value at this pressure. The

mobility of the oil will increase with decreasing oil viscosity, which in turns improves the sweep efficiency [2].

1.3.2 Free gas saturation

In many oil reservoirs, a free-gas saturation formed during the early production period because the water flood was not initiated before the reservoir pressure had dropped through the oil bubble point pressure. The increase in the value of free gas saturation will decrease the residual oil that is trapped in the rock.

In water injection projects, it is desirable to have initial gas saturation, possibly as much as 10%. This will occur at a pressure that is below the bubble point pressure. In gas injection projects, zero gas saturation in the oil zone is desired. This occurs while reservoir pressure is at or above bubble point pressure [2].

1.3.3 Cost of injection equipment

This is related to reservoir pressure and at higher pressures, the cost of injection equipment increases. Therefore, a low reservoir pressure at initiation of injection is desirable [2].

1.3.4 Productivity of producing wells

A high reservoir pressure is desirable to increase the productivity of producing wells, which prolongs the flowing period of the wells; decreasing lifting costs and mat shorten the overall life of the project [2].

1.3.5 Overall life of the reservoir

Because operating expenses are an important part of total cost, the fluid injection process should be started as early as possible [2].

1.4 Selection of flooding pattern

One of the first steps of designing a water flooding project is flood pattern selection. The objective is to select the proper pattern that will provide the injection fluid with the maximum possible contact with the crude oil system. This selection can be achieved by converting some existing production wells into injectors or drilling infill injection wells. Different factors must be taken into consideration when making the selection:

1. Reservoir heterogeneity
2. Direction of formation fractures
3. Availability of the injection fluid
4. Desired and anticipated flood life
5. Maximum oil recovery
6. Well spacing, productivity, and injectivity [2].

The selection of a suitable flooding pattern for the reservoir depends on the number and location of existing wells. In some cases, producing wells can be converted to injection wells while in other cases it may be necessary to drill new injection wells. There are different types of well arrangement that are used in fluid injection projects and the following are two of them:

1.4.1 Peripheral injection patterns

In peripheral injection, the injection wells are located at the external boundary of the reservoir and the oil is displaced toward the interior of the reservoir as shown in Figure 1.1 which points out the following main characteristics of the flood as it yields a maximum oil recovery with a minimum of produced water. In addition, the production of significant quantities of water can be delayed until only the last row of producer's remains. Moreover, for a successful flood, the formation permeability should be large enough to permit the movement of the injected water at the desired rate over the distance of several well spacing from injection wells to the last line of producers. In general, this type of well arrangement is favorable in homogeneous reservoir with high permeability.

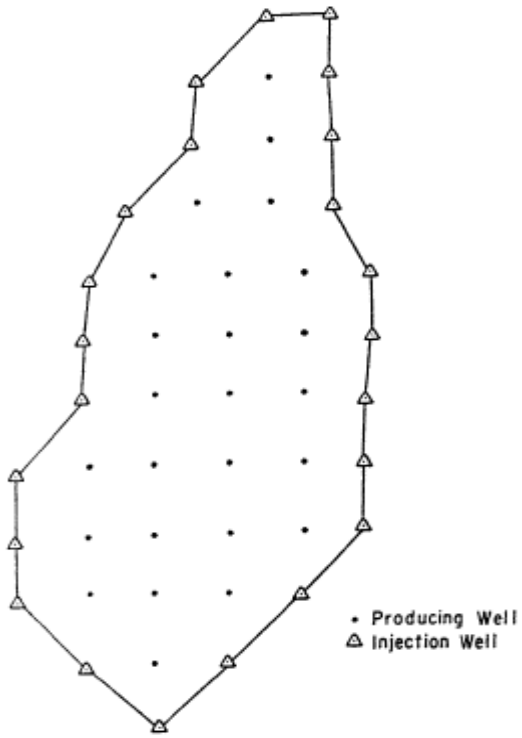

Figure 1.1: Peripheral injection patterns

1.4.2 Pattern injection

Due to the fact that oil leases are divided into squares miles and quarter square miles, fields are developed in a very regular pattern as shown in Figure 1.2. A wide variety of injection-production well arrangement have been used in injection projects. This type of well arrangement is favorable for heterogeneous reservoirs (block faulted).

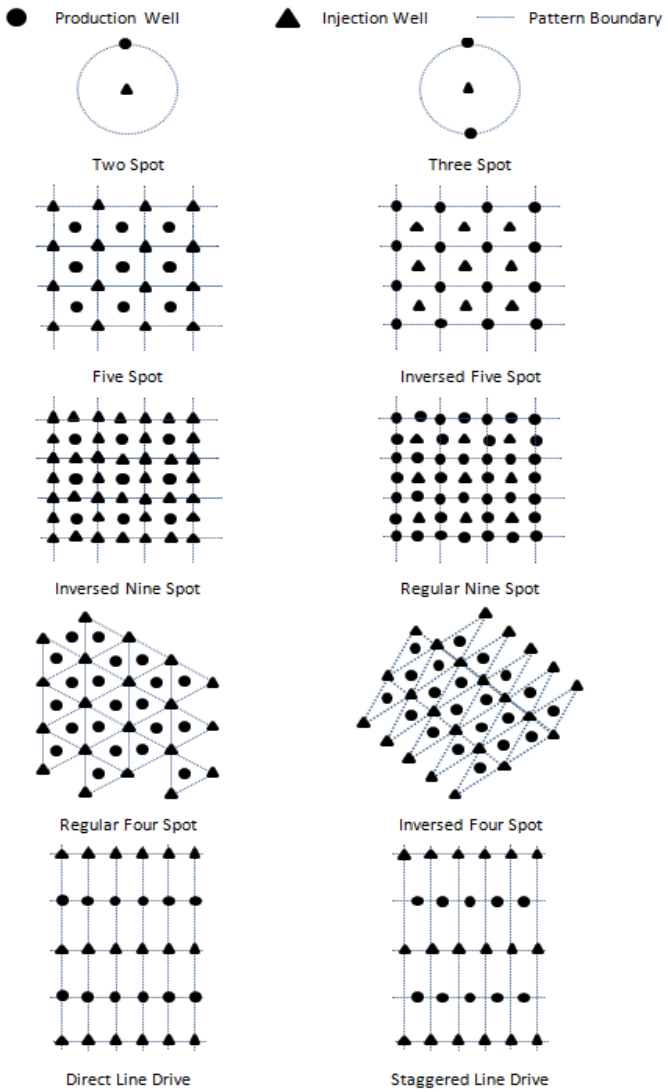

Figure 1.2: Types of flood pattern

The flood pattern that was used in this project is the 5-spot flood pattern. It is a special case of staggered line drive in which the distance between all like wells is constant. Any four-injection wells thus form a square with a production well at the center.

1.5 Overall recovery efficiency

The overall recovery factor of any secondary or tertiary oil recovery method is the product of a combination of three individual efficiency factors as given by Equation 1.1:

$$RF = E_D E_A E_V \tag{1.1}$$

The displacement efficiency is the fraction of movable oil that has been displaced from the swept zone at any given time or pore volume injected. Because an immiscible gas injection or water flood will always leave behind some residual oil, E_D will always be less than 1.

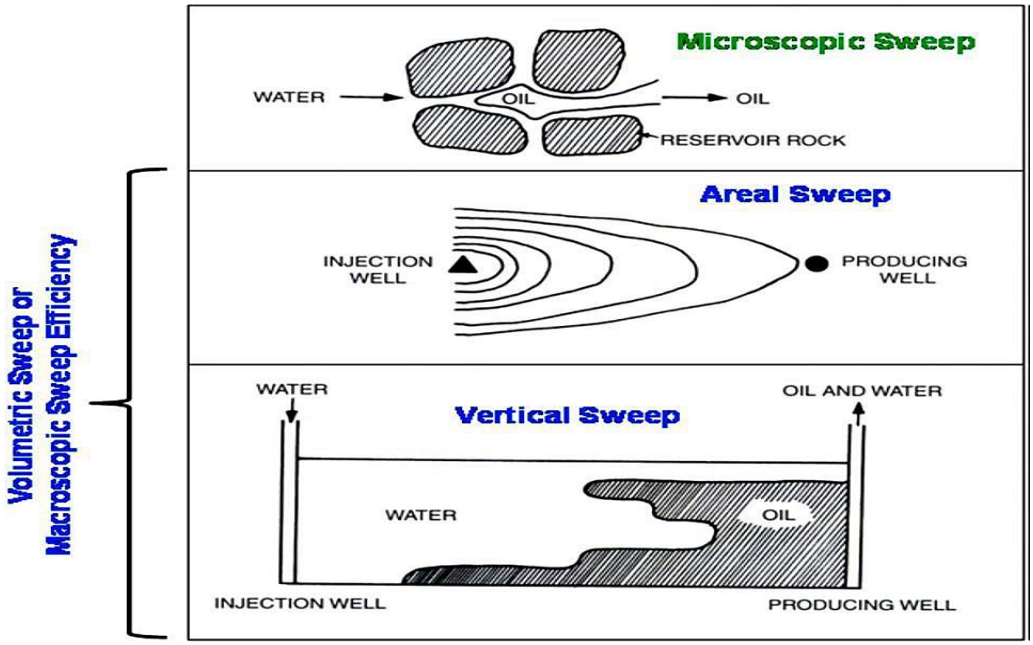

Figure 1.3: Microscopic and macroscopic sweep efficiency

The areal sweep efficiency is the fractional area of the pattern that is swept by the displacing fluid as shown in Figure 1.3. The major factors determining areal sweep are:

1- Fluid mobility
2- Pattern type
3- Areal heterogeneity
4- Total volume of fluid injected

The vertical sweep efficiency is the fraction of the vertical section of the pay zone that is contacted by injected fluids. The vertical sweep efficiency is primarily a function of:

1- Vertical heterogeneity
2- Degree of gravity segregation
3- Fluid mobility
4- Total volume injection

The product of $E_A E_V$ is called the volumetric sweep efficiency and represents the overall fraction of the flood pattern that is contacted by the injected fluid. In general, reservoir heterogeneity probably has more influence than any other factor on the performance of a secondary or tertiary injection project. The most important two types of heterogeneity affecting sweep efficiencies, E_A and E_V, are the areal reservoir heterogeneity and vertical heterogeneity, respectively [2].

1.6 Displacement performance

Under ideal conditions, water would displace oil from pores in a rock in a piston-like manner or at least in a manner representing a leaky piston. However, because of various wetting conditions, relative permeability of water and oil are important in determining where flow of each fluid occurs, and the manner in which oil is displaced by water. In addition, higher viscosity of crude oil in comparison to water will contribute to non-ideal displacement behavior and thus the piston-like displacement will be altered to take other forms [3].

In general, if the mobility is equal to or less than one, this is a very favorable condition because there is no tendency for the water to bypass the oil. The displacement is considered unconditionally stable and it is characterized by piston-like displacement in flooded reservoirs with crossflow such that a balance between gravity and injection rate is achieved.

1.7 The purpose of the present work

The main objective of this work is to develop an easy to use, new formula for predicting oil recovery in layered reservoirs subjected to water flooding. Other objectives include gaining hands-on experience with (1) the industry-standard reservoir simulator known as ECLIPSE and (2) the Minitab and specifically the non-linear regression analysis simulator. Finally, yet importantly is to add a useful predictive tool in the mature subject of secondary oil recovery.

Chapter 2: Literature Review

Predicting water flooding performance has been discussed by many published models and different authors are trying to generate an approach that predict the best fit model which gives the most reasonable or reliable performance comparing with injection projects. Here are some published models for water flooding performance:

2.1 Guthrie-Greenberger method

In the past, empirical correlations for prediction of recovery factor performance were investigated by statistical study of recovery factor performances. Guthrie and Greenberger studied oil recovery by water drive empirically to reservoir rock and fluid properties. They studied 73 sandstone reservoirs that had a water drive or that had solution gas drive combined with a water drive. The actual production data were available for these reservoirs. The oil recovery was related to the permeability, porosity, oil viscosity, formation thickness, connate water saturation, depth, oil reservoir volume factor, area, and well spacing. The correlation shown below fits so well that in 50% of the time the recovery factor was within 6.2% of the reported value, and in 75% of the time it was within 9.0%. This equation implies that the water drive recovery efficiency is lower in reservoirs of higher porosity [4].

$$E_R = 0.2719 \log k + 0.25569 S_{wi} - 0.1355 \log \mu_o - 1.5380 \phi - 0.0003488 h + 0.114403 \quad (2.1)$$

In this correlation, E_R is the fractional recovery efficiency, k is the absolute permeability in md, S_{wi} is the initial water saturation, ϕ is the porosity, h is the formation

thickness in ft and μ_o is the oil viscosity in cP. This equation implies that the water drive recovery efficiency is lower in reservoirs of higher porosity.

2.2 API statistical study

The API sub-committee on Recovery Efficiency, headed by Arps [14] presented a statistical study of recovery efficiency based on a statistical analysis of data from 312 reservoirs. They developed correlations for water drive recovery from sandstone and sand reservoirs, and for solution gas drive reservoirs from sandstones, sands, and carbonates. The water drive recovery, as a percentage of the original oil in place. This correlation for water drive recovery is expressed as a logarithmic-type equation. The correlation coefficient for the equation is 0.958, which by its closeness to 1.000 shows a very good fit of the data. This correlation developed from a water drive reservoir performance data has limited usefulness for recovery factor utilizations. The usefulness of this type of correlation is generally limited to reservoirs in the particular geographical area being studied [4].

$$ER = 54.898 \left[\frac{Ø\,(1-Swi)}{Boi}\right]^{0.0422} \left[\frac{K\,\mu w}{\mu o}\right]^{0.077} (S_{wi})^{-0.1903} \left[\frac{Pi}{Pa}\right]^{-0.2159} \quad (2.2)$$

In this correlation, E_R is the recovery factor, ϕ is the porosity, μ_w is the water viscosity in cP, μ_o is the oil viscosity in cP, k is the absolute permeability in md, S_{wi} is the initial water saturation, p_i is the initial pressure in psia, p_a is the pressure at depletion (abandonment pressure) in psia and B_{oi} is the oil formation volume factor in rb/stb.

2.3 Empirical correlation method

The approach used for the development of the Empirical Correlation Method (ECM) relies on dividing the flood performance into time periods. However, the previous work is extended to include a quantitative measure of the effect of fluid and rock properties on the performance of a flood. The following reservoir and rock properties were found to have statistically significant influence on flood behavior: (1) permeability variations; (2) oil and gas saturation at the start of the flood; (3) oil-water viscosity ratio; (4) injection rate; arid (5) an average distance from first-line producers. The ECM is based on a statistical analysis of actual water flood performance of eight Southern California floods.

The limitation is since the ECM is based on data from only eight Southern California floods, there may be cases when meaningless values are generated for some of the parameters defining the flood performance curve, even though the correlations are statistically very significant. For the best use of the ECM, it is recommended that the correlations be applied to those depleted or semi depleted reservoirs having fluid and rock properties that fall within the range of data used for the development of this method. Also, the method may be applicable only locally in California [5].

2.4 Statistical secondary recovery model

A secondary recovery model has been developed to predict water flood performance for different reservoir properties and design conditions. A causal model based on simple and multiple regression equations uses eight input variables to estimate injection rate, ultimate secondary reserves, response time and yields peak oil rate, peak year and the production profile as a function of time. It is used for secondary reserve

booking, to develop production profiles for project economics and authorization for expenditures and to assess technical risk by means of the simulation technique.

This novel approach relies on historical data from 12 water floods located in the San Jorge Basin, but can be used in other areas once the regression coefficients for the particular reservoirs are estimated. This causal statistical model predicts water flood performance for different reservoir properties and design conditions, with a set of equations developed using simple and multiple regression. They were developed by omitting those variables with no significant effect, estimating the regression coefficients, finding the most effective prediction equations and determining their strength by correlation analysis. The model employs six geometrical factors and two reservoir quality parameters to generate five output variables. Input variables are reservoir depth, total net sand thickness, pore volume, number of sand layers, number of injectors and producers, porosity and primary recovery factor. Output variables include injectivity, secondary recovery factor, response time, project life and recovered reserves after injecting 28 percent of the required number of pore volumes (R28). By applying these output variables, the injection rate, secondary recovery, number of pore volumes to inject to recover the ultimate secondary reserves, peak oil rate and year and the production profile as a function of time are been estimated [6].

2.5 New correlation to predict water flood performance

Recently, a new correlation was proposed for estimating oil recovery factor under water flooding in core samples at constant water injection rate [16]. The coefficients and powers of parameters were determined using a non-linear regression. The correlation depends on the dimensionless temperatures and fluid properties defined in Equation (2.3).

$$RF = [(0.165 \ln (Tr/Ts) * 0.88) + (0.0066 \ln (\mu o/\mu w)) + (0.280 \ln (1/\Upsilon o) * 1.55)] + 0.26 \quad (2.3)$$

Where, *RF* is the recovery factor, %, Tr is the reservoir temperature, °F, Ts is the surface temperature, °F, μ_o is the oil viscosity, cP, μ_w is the water viscosity, cP, Υo is the oil specific gravity. The authors observed that oil recovery factor increased up to 48.8% at 194°F, compared to 38% at 95°F when one pore volume was injected. In addition, their results showed that the proposed correlation is reliable when compared with three sandstone reservoirs in Libya and one sandstone reservoir in Kuwait.

2.6 Estimation of oil recovery factor using artificial intelligence

Very recently, the artificial intelligence approach was used to estimate oil recovery factor in water flooded reservoirs [15]. In their study, the authors collected a dataset of 173 lessons and analyzed it statistically. The outliers were removed based on the standard deviation (SD) where any data point out of the range of ± 0.3 SD was considered as an outlier. Five lessons were removed from the data based on the SD criteria. Then, the remaining dataset (168 lessons) were used to develop the AI models. These models were trained using 77% of the data, and the remaining (23%) were used to test the trained models. These parameters could be divided into four groups (asset size, rock

parameters, fluid properties, and reservoir energy). The authors claimed that their equation outperformed the available equations in terms of all the measures of error evaluation considered in their study, and also has the highest coefficient of determination of 0.94 compared to only 0.55 obtained from Gulstad correlation [17], which they considered as one of the most accurate correlations currently available.

Chapter 3: Methodology of Simulation Model and Preparation of Input Data

3.1 ECLIPSE simulator

ECLIPSE is an oil and gas reservoir simulator originally developed by ECL (Exploration Consultants Limited) and currently owned, developed, marketed and maintained by SIS (formerly known as GeoQuest), a division of Schlumberger. The name ECLIPSE originally was an acronym for "ECL´s Implicit Program for Simulation Engineering".

The ECLIPSE industry-reference simulator offers the industry's most complete and robust set of numerical solutions for fast and accurate prediction of dynamic behavior for all types of reservoirs and development schemes. The ECLIPSE simulator has been the benchmark for commercial reservoir simulation for more than 25 years thanks to its extensive capabilities, robustness, speed, parallel scalability, and unmatched platform coverage. ECLIPSE 100 can be used to simulate 1, 2 or 3 phase systems. Two-phase options (oil/water, oil/gas, and gas/water) are solved as two component systems saving both computer storage and computer time. In addition, to gas dissolving in oil (variable bubble point pressure or gas/oil ratio), ECLIPSE 100 may also be used to model oil vaporizing in gas (variable dew point pressure or oil/gas ratio) [7].

3.1.1 Data organization

An Eclipse data file is comprised of eight sections headed by a section header (Some of the sections are optional). These sections must come in the prescribed order, but the order of the keywords within each section is arbitrary (except the SCHEDULE section

where time-dependency is handled in the order it is defined). The data sections, with headers, are:

RUNSPEC (required)

Run specifications. Includes a description of the run, such as grid size, table sizes, number of wells, which phases to include and so forth.

GRID (required)

Defines the grid dimensions and shape, including petro physics (porosity, permeability, net-to gross).

EDIT (optional)

User-defined changes to the grid data which are applied after Eclipse has processed them, can be defined in this section.

PROPS (required)

Fluid and rock properties (relative permeability, PVT tables, etc.)

REGIONS (optional)

User defined report regions, or e.g. regions where different relative-permeability curves apply can be defined in this section.

SOLUTION (required)

Equilibration data (description of how the model is to be initialized).

SUMMARY (optional)

Results output is primarily of two types:

1) Scalar data as a function of time (e.g. average field pressure).

2) Data with one value pr. grid cell (e.g. oil saturation). These are only output at chosen times.

This section is used to define output of the first kind, by specifying which data items to write to report files.

SCHEDULE (required)

Well definitions, description of operating schedule, convergence control, and control of output of the second kind described above [8].

3.2 Data preparation for simulator

3.2.1 Permeability variation across reservoir (Reservoir Heterogeneity)

The Dykstra-Parsons correlation was used to generate permeability distribution across reservoir thickness. This part is important because it helps getting the permeability value for each layer of the reservoir with different variation of heterogeneity. In practice, the permeability variation is determined by arranging the permeabilities in descending order and determining the percent-greater-than values for each permeability. From a plot of k versus percent greater than on a log probability graph sheet, the values of k at 50% and k at 84.1% are read, and V is determined by Equation 3.1:

$$V = (k_{50} - k_{84.1}) / k_{50} \quad (3.1)$$

Equation 3.1 has been rearranged to get the value of $k_{84.1}$ at different heterogeneities and its shown using Equation 3.2 and the results are presented in Table 3.1:

$$k_{84.1} = k_{50} (1\text{-}V) \quad (3.2)$$

Table 3.1: Values of k50 and k84.1

V	k_{50} (md)	$k_{84.1}$(md)
0.1	68	61.2
0.3	68	47.6
0.5	68	34
0.7	68	20.4

The permeability variation was plotted using data in table so that it shows the value of k_{50} is fixed for all cases and only changing the value of $k_{84.1}$ so that each case of heterogeneity is shown in Figure 3.1. This plot was used to read the values of permeability variation for the 10 layers for all values of heterogeneity.

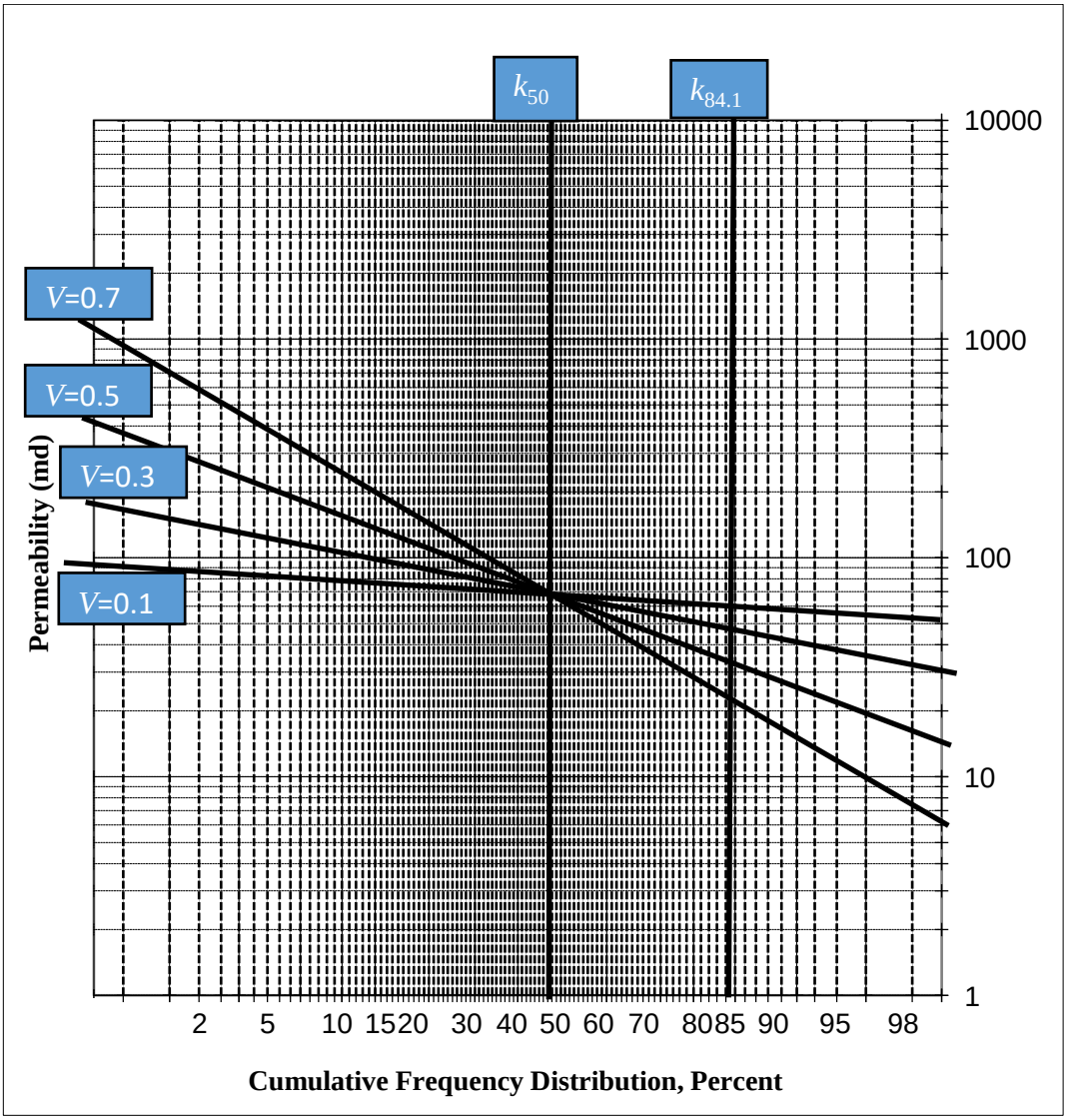

Figure 3.1: Dykstra Parsons permeability variation plot for V = 0.1 up to 0.7

The results of calculations of k_{50} and $k_{84.1}$ listed in Table 3.1 were implemented to generate the relationships for various values of *V* as shown in Figure 3.1. The permeability distributions for the 10 layers were then extracted from Figure 3.1 and the results are listed in Table 3.2.

Table 3.2: Permeability distribution

k, md			
V= 0.1	*V*= 0.3	*V*= 0.5	*V*= 0.7
78	130	190	400
76	110	160	300
74	97	130	220
73	93	120	170
71	87	110	140
70	84	95	130
69	78	87	105
68	75	78	87
67	72	72	75
66	68	65	65

3.2.2 Generation of relative permeability curve using Corey's correlations.

This is critical because it assigns the system to be either oil wet or water wet. In this work, Corey's correlations, Equation 3.3 and Equation 3.4, were implemented to generate the relative permeability curves and the results of calculations are presented in Table 3.3 and Figure 3.2. The calculations were done using the following correlations:

$$k_{ro} = [(1-S_w) / (1- S_{wi})]^4 \quad (3.3)$$

$$k_{rw} = [(S_w- S_{wi}) / (1- S_{wi})]^4 \quad (3.4)$$

Sample calculation for the next table:

@ $S_w = 0.5$ and $S_{wi} = 0.3$

$k_{ro} = [(1-S_w) / (1- S_{wi})]^4 = [(1-0.5) / (1- 0.3)]^4 = 0.2603$

$k_{rw} = [(S_w- S_{wi}) / (1- S_{wi})]^4 = [(0.5- 0.3) / (1- 0.3)]^4 = 0.0067$

Table 3.3: Relative permeability data

S_w	k_{ro}	k_{rw}
0.30	1	0
0.35	0.743466	2.6E-05
0.40	0.539775	0.000416
0.45	0.381117	0.002108
0.50	0.260308	0.006664
0.55	0.170788	0.016269
0.60	0.106622	0.033736
0.65	0.062500	0.062500
0.70	0.033736	0.106622
0.75	0.016269	0.170788
0.80	0.006664	0.260308

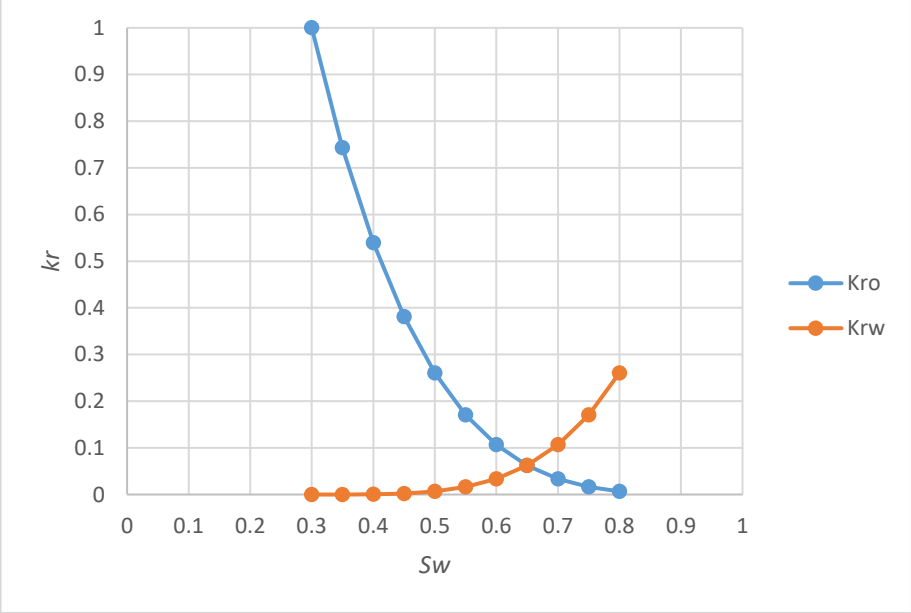

Figure 3.2: Relative permeability curves generated by Corey's correlations.

3.2.3 Assumed input data and basic assumptions

Additional input data for the simulator were necessary to enable the generation of various recovery performances for various scenarios. The assumed data are listed in Table 3.4 and Table 3.5.

Table 3.4: Eclipse input data

Parameter	Value
Number of cells in x-direction	10
Number of cells in y-direction	10
Number of layers	10
Depth	8,000 ft
Pressure	4,500 psia
Temperature	240 F
Thickness	50 ft
Area	72 acres
Porosity	0.20
Water formation volume factor	1.02 rb/stb
Water viscosity	0.75 cP
Water compressibility	$3*10^{-6}$ psi^{-1}
Water density	49 lbs/cf
Oil density	63 lbs/cf
Gas density	0.01 lbs/cf
Pore compaction	$4*10^{-6}$ psi^{-1}
Water oil Contact	8,050 ft

Table 3.5: Oil PVT data, bubble point pressure (p_b) = 300 psia

p (psia)	Bo (rb/stb)	μ_o (cP)
300	1.25	1.0
800	1.20	1.1
6,000	1.15	2.0

Table 3.5 is needed as input for Eclipse software as more than one value of *Bo* will be used in the calculation. Eclipse linearly interpolates the reciprocals of *Bo* and (*Bo* μo) between data points, rather than the values themselves. This should be taken into account when comparing the results of ECLIPSE with those of other simulators, by ensuring the data points are not distributed too sparsely.

The basic assumptions made in this work as follows:

1- Water wet reservoir.
2- No free gas saturation at all time during flood.
3- One quadrant of five spot pattern; as shown in Figure 3.3 where x is length of square side.
4- Neglect capillary pressure effect.
5- Layered reservoir with log normal permeability distribution.
6- Constant porosity, thickness and initial water saturation for all layers.
7- Low volatility of black oil.

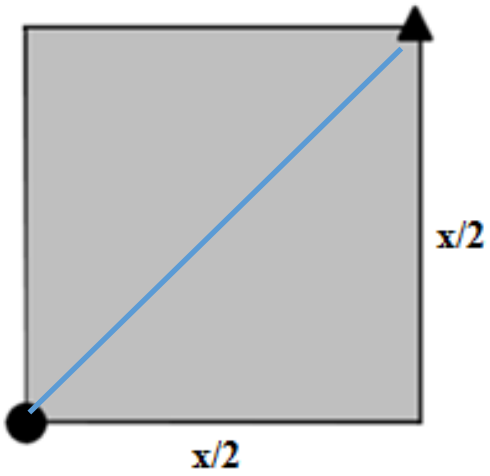

Figure 3.3: A quadrant of five spot pattern.

3.3 Combination scenarios of various key parameters

The Eclipse simulator was used to generate production performance profiles for various combination scenarios. Four key parameters of dominant impact in water flooding projects were considered in this work. These parameters are water injection rate, water viscosity, reservoir anisotropy and reservoir heterogeneity. Table 3.6 presents values of key parameters used in the combination scenarios. Consequently, the total number of scenarios resulted from these combinations was 192.

Table 3.6: Values of key parameters used in the Combination Scenarios

Variables	Scenarios
Reservoir Heterogeneity	V = 0.1; 0.3; 0.5 and 0.7
Water Injection Rate	q_i = 2,000; 5,000 and 10,000 stb/d
Permeability Anisotropy	kz/kx = 0.1; 0.3; 0.5 and 1
Water Viscosity	μ_w = 0.25; 0.5; 0.75 and 1 cP

3.4 Generation of simulation data for statistical analysis.

In addition to other performance profiles, the main output from eclipse after running the above combination scenarios are the water cut versus time and the oil recovery factor versus time. The results of the simulator output are shown in Table A.1 of Appendix A.

3.5 Application of minitab to develop the new empirical correlation.

The simulator-generated data were then used as input data for the Minitab software for further statistical analysis. The objective of using Minitab software is to generate the proposed empirical correlation for oil recovery factor in terms of the key parameters listed in Table 3.6. The General Linear Model was used especially because it predicts values for new observations, identify the combination of predictor values that jointly optimize one or more fitted values, and create surface plots, contour plots, and factorial plots. Also, it can signify the key parameters of greater impact on the recovery of oil in water flooded reservoirs and shows the one with the most effect and the one with the least effect.

3.6 Validation of the new empirical correlation

The empirical correlation (s) thus developed by the Minitab software using the simulator-generated data were then validated using data outside the range of those used in their development. Figure 3.4 illustrates the methodology adopted in this work.

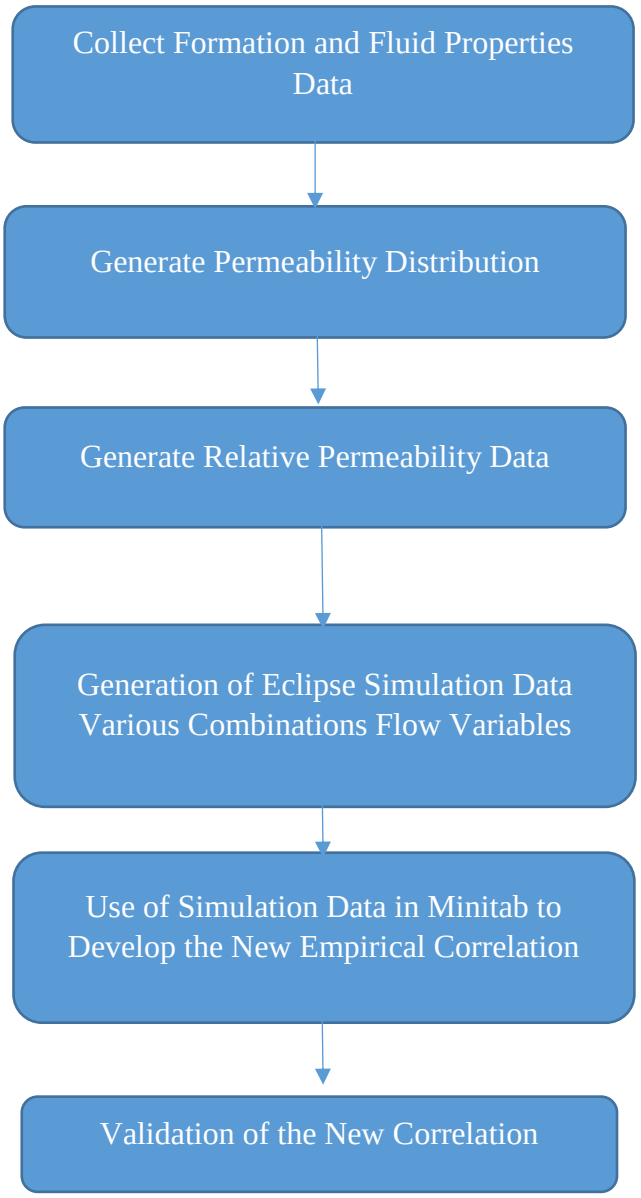

Figure 3.4: Methodology flow chart.

Chapter 4: Results of Simulation

The simulation-generated data for the 192-combination scenarios are listed in Tables A.1. Plots of specific performances for selected combination scenarios are shown in Figure 4.1 through Figure 4.16. These plots show the simulated performances of pressure, oil recovery factor, water cut and cumulative oil produced during the water flooding project.

4.1 Effect of water viscosity

Selected combination scenario:

V = 0.5, k_z/k_x = 1, q_i = 10,000 stb/day and μ_w = 0.25-1 cP

This selected scenario investigates the effect of changing water viscosity on the water flood performance. In this scenario, all parameters were held constant and only water viscosity was changing and the results of the various performances are shown in Figure 4.1 through 4.4. As can be observed from these plots, the most effective case is when the water viscosity approaches the oil viscosity because it leads to favorable mobility ratio of one or less than one. Under such conditions the highest cumulative oil production of nearly 35 MMstb has been achieved as indicated in Figure 4.4, and corresponding RF of 45% as shown in Figure 4.2, at end of project. In addition, a water viscosity of 1 cP, which yields favorable mobility ratio, has been found to yield later breakthrough time and lower water cut than those predicted for the lower water viscosities as shown in Figure 4.3. Thus, favorable mobility ratio can be achieved as the water

viscosity approaches the oil viscosity resulting in improved overall water flooding performance.

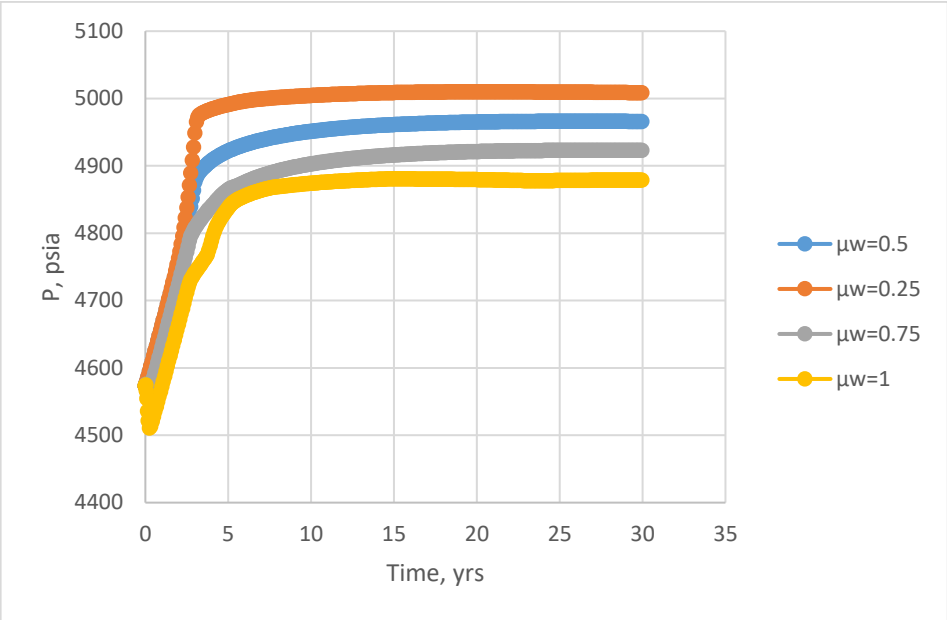

Figure 4.1: Field average pressure performance (Case 1)

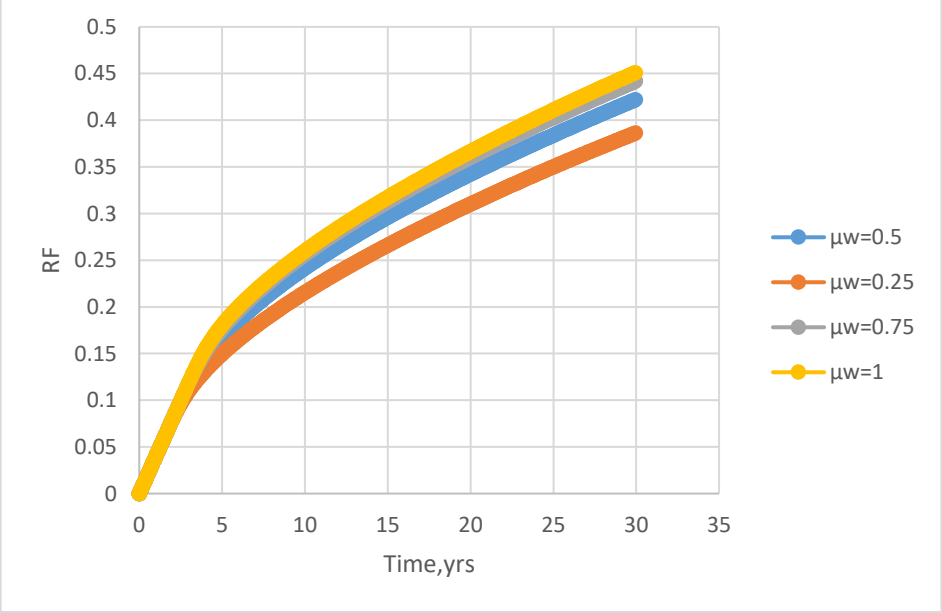

Figure 4.2: Oil recovery factor performance (Case 1)

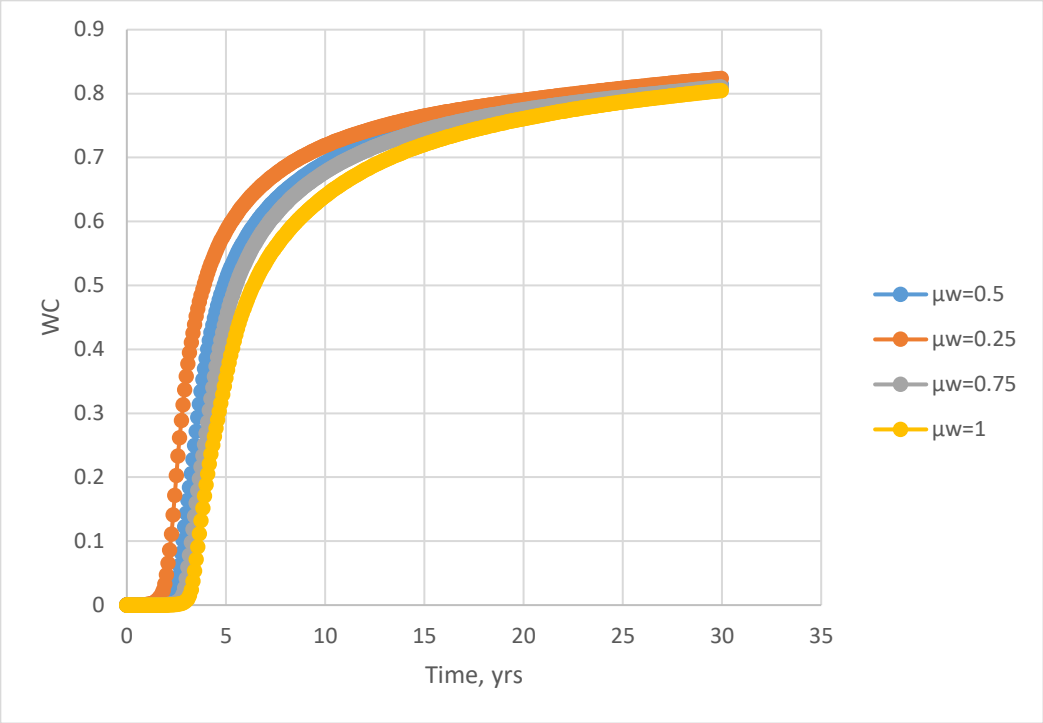

Figure 4.3: Water cut performance (Case 1)

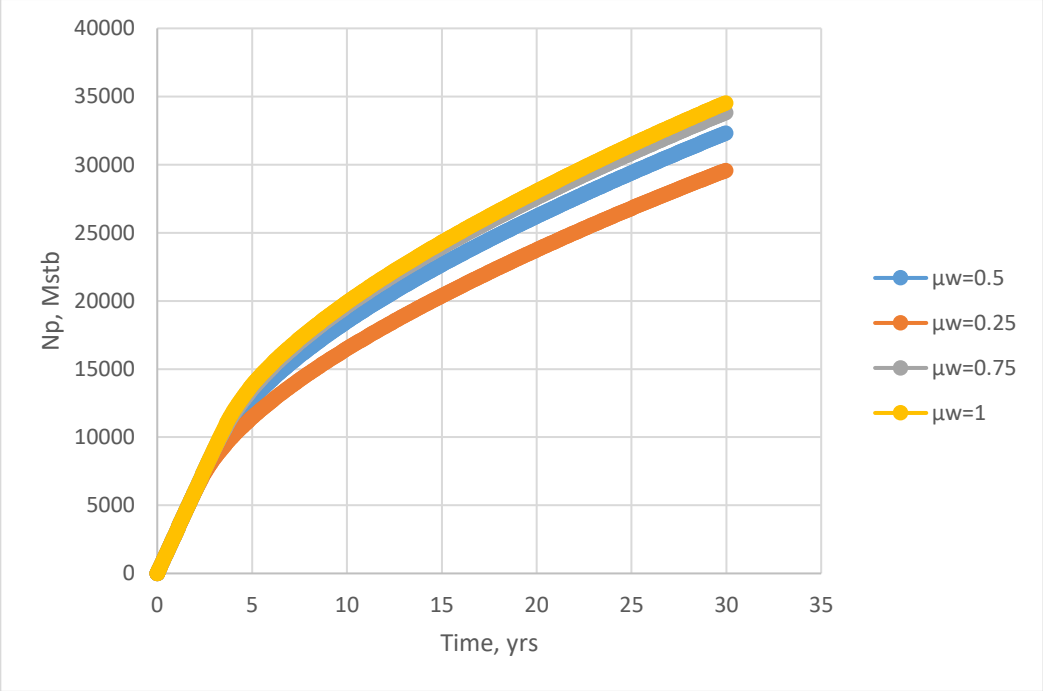

Figure 4.4: Cumulative production performance (Case 1)

4.2 Effect of water injection rate

Selected combination scenario:

V = 0.7, k_z/k_x = 1, μ_w = 1 cP and q_i= 2,000 - 10,000 stb/day

In this scenario, the effects of water injection rate on the average field pressure, water cut, and oil recovery factor were investigated, as illustrated in Figures 4.5 through 4.8. In these plots, the water injection rate was changed between 2,000 stb/d and 10,000 stb/d. The injection pressure performance plot, Figure 4.5, clearly shows that increasing water injection rate would lead to faster pressure maintenance which is one of two main goals usually achieved in water flooding schemes. The significance of injecting water at high rates is also realized in Figures 4.6 and 4.7. The oil recovery factor was increased from 23% to 51% as the water injection increased from 2,000 stb/d to 10,000 stb/d and as shown in Figure 4.6. The negative aspect of injecting water at high rate, however, is revealed in Figure 4.7, as it yields earlier water breakthrough at the producing end and significant increase of the produced water cut. This negative aspect of high-water injection rate of 10,000 stb/d may well be counter balanced by the significant increase of cumulative oil production of around 40 million stb at the end of the project as shown in Figure 4.8. Therefore, the feasibility of any water flooding project should be assessed based on similar performances as described above, and the final decision would be a compromise of the above effects.

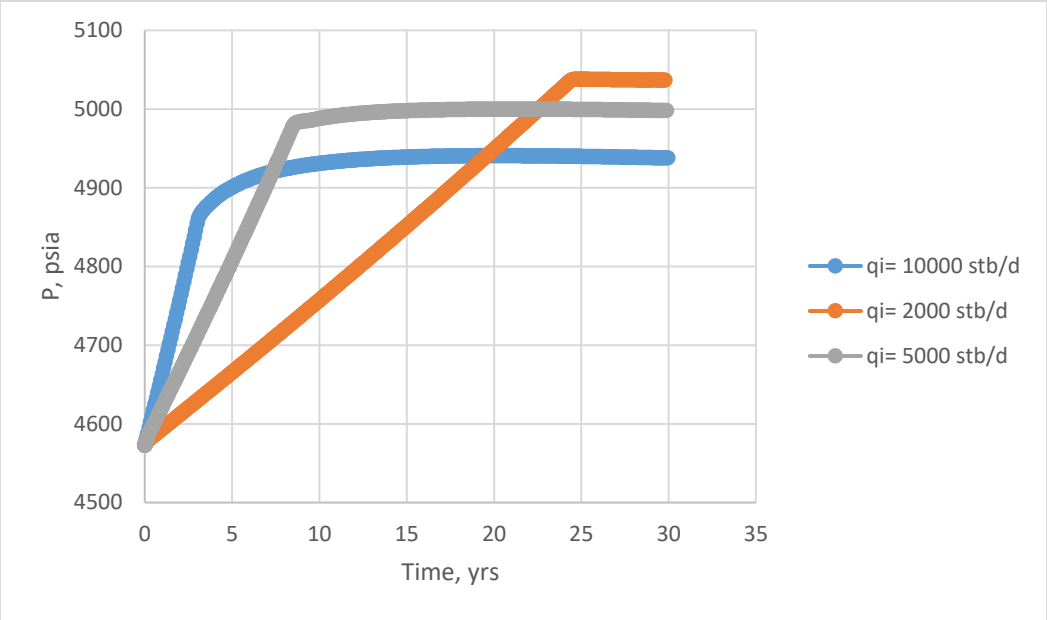

Figure 4.5: Field average pressure performance (Case 2)

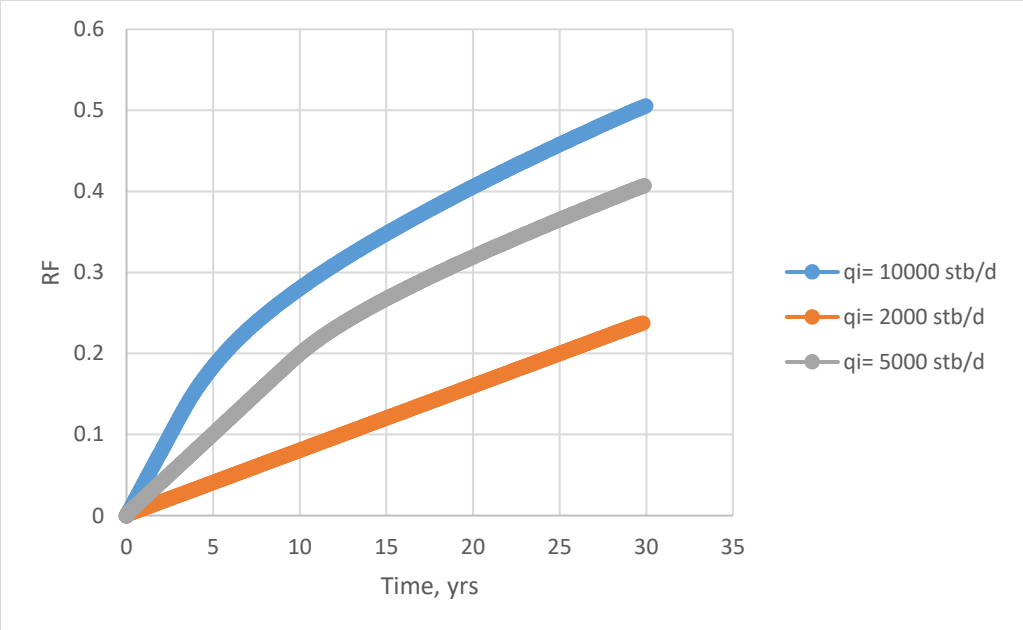

Figure 4.6: Oil recovery factor performance (Case 2)

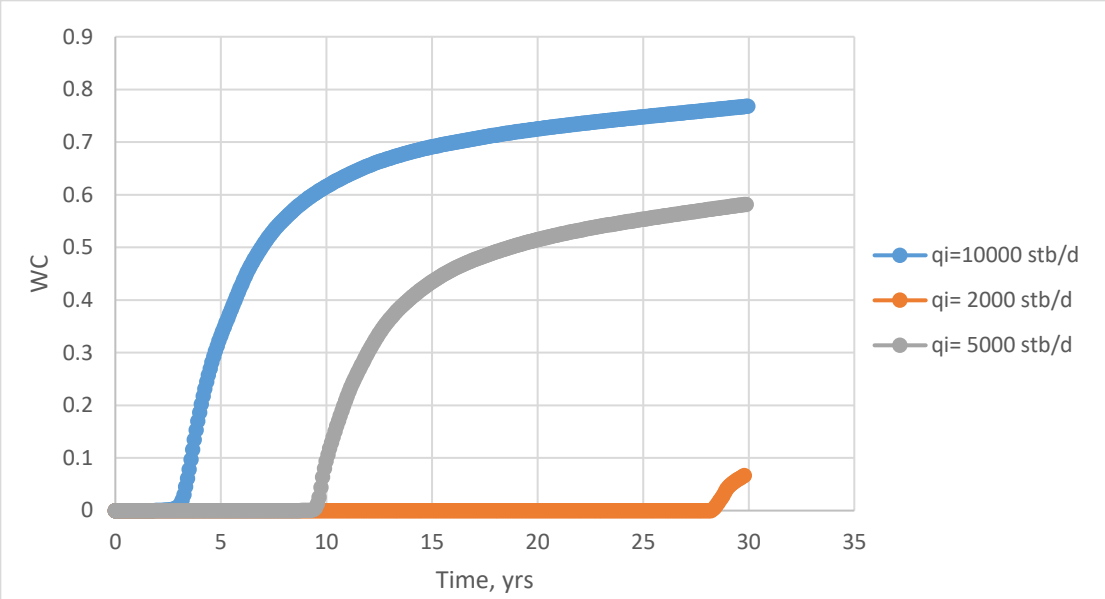

Figure 4.7: Water cut performance (Case 2)

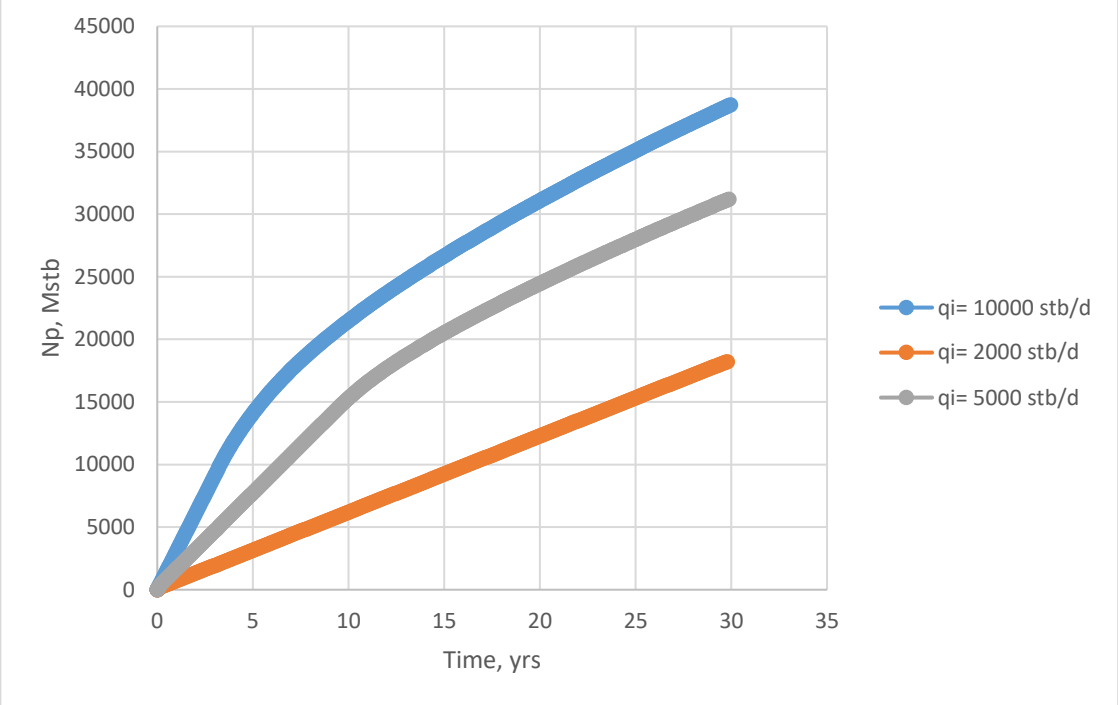

Figure 4.8: Cumulative production performance (Case 2)

4.3 Effect of reservoir heterogeneity

Selected combination scenario:

$k_z/k_x = 1$, $\mu_w = 0.5$ cP, $q_i = 10{,}000$ stb/day and V = 0.1 - 0.7

In this scenario, the effects of changing permeability variation coefficient on water flooding performance were investigated and the results are plotted in Figure 4.9 through 4.12. In these plots *V* was varied between 0.1 and 0.7 and other parameters were held constants to observe the significance of reservoir heterogeneity on water flooding performances. It can be observed from Figure 4.10 that a coefficient of 0.1 gives the highest RF which reaches 46% and that is the homogeneous case. On the other hand, when the coefficient is 0.7, which is a heterogeneous reservoir, RF is only 33%. Figure 4.12 confirms the significance of this parameter as the cumulative production increases from 24 MMstb to 38 MMstb for *V* values of 0.7 and 0.1, respectively. Similar observations of improved performances can be realized in Figure 4.9 and Figure 4.11. Therefore, homogeneous reservoirs are favorable in water flood schemes.

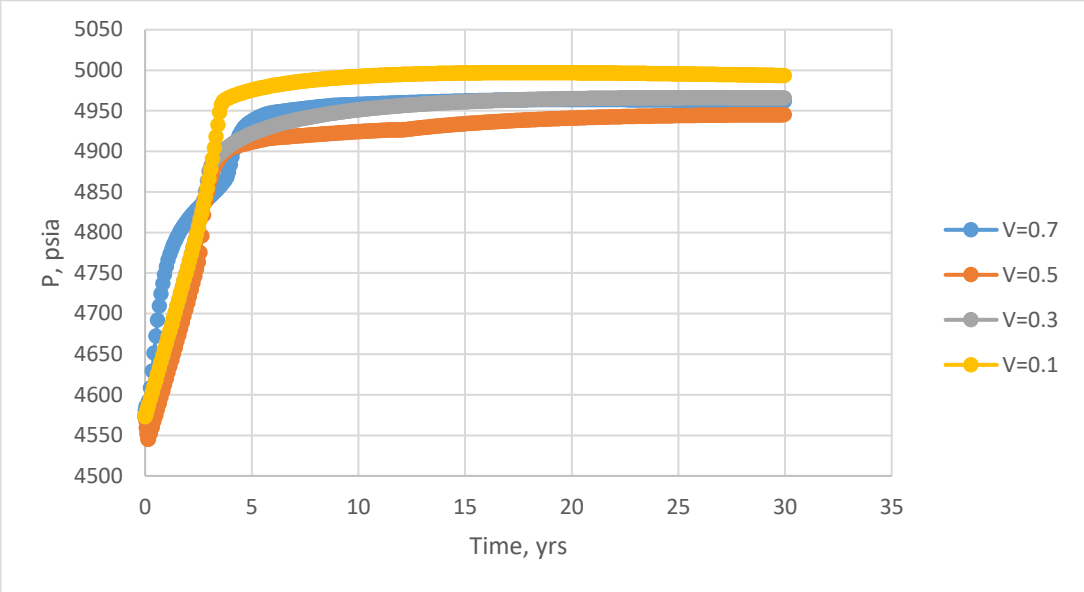

Figure 4.9: Average field pressure performance (Case 3)

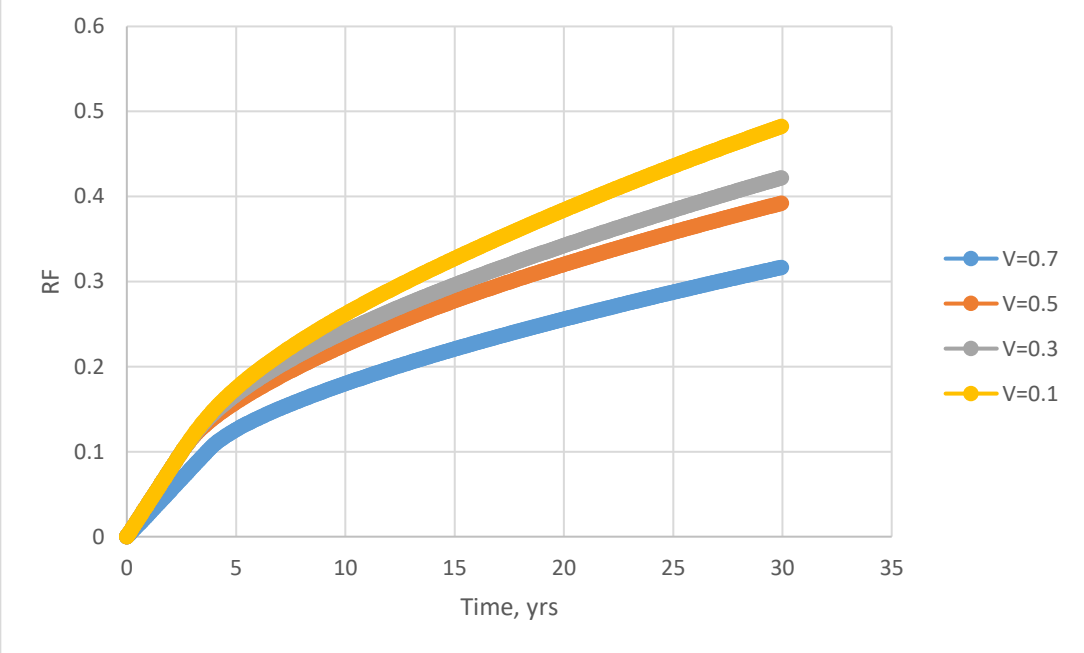

Figure 4.10: Oil recovery factor performance (Case 3)

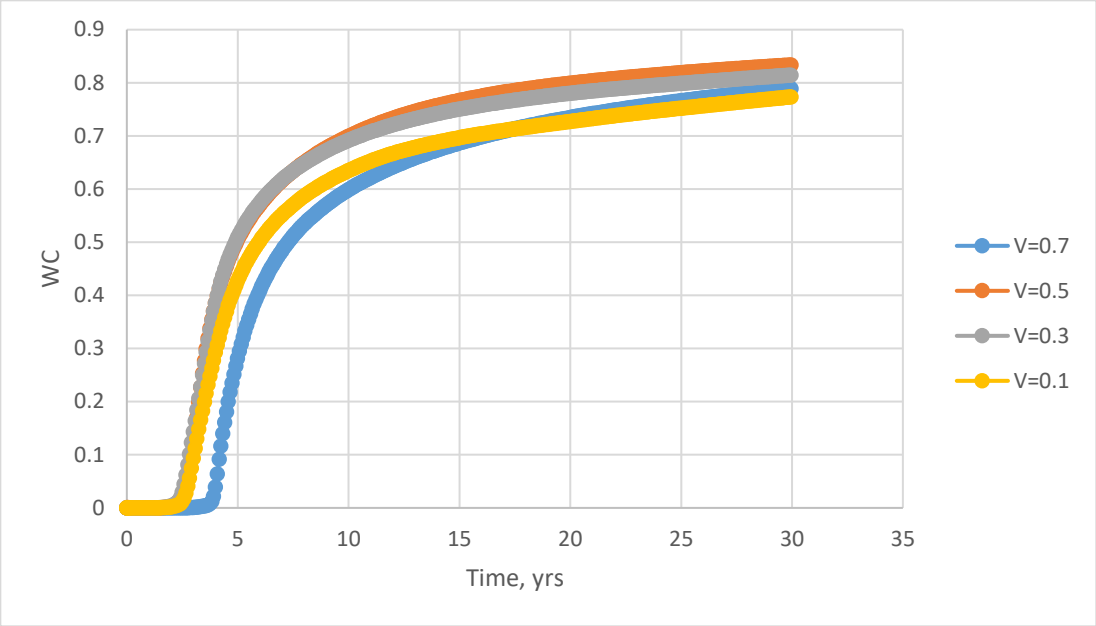

Figure 4.11: Water cut performance (Case 3)

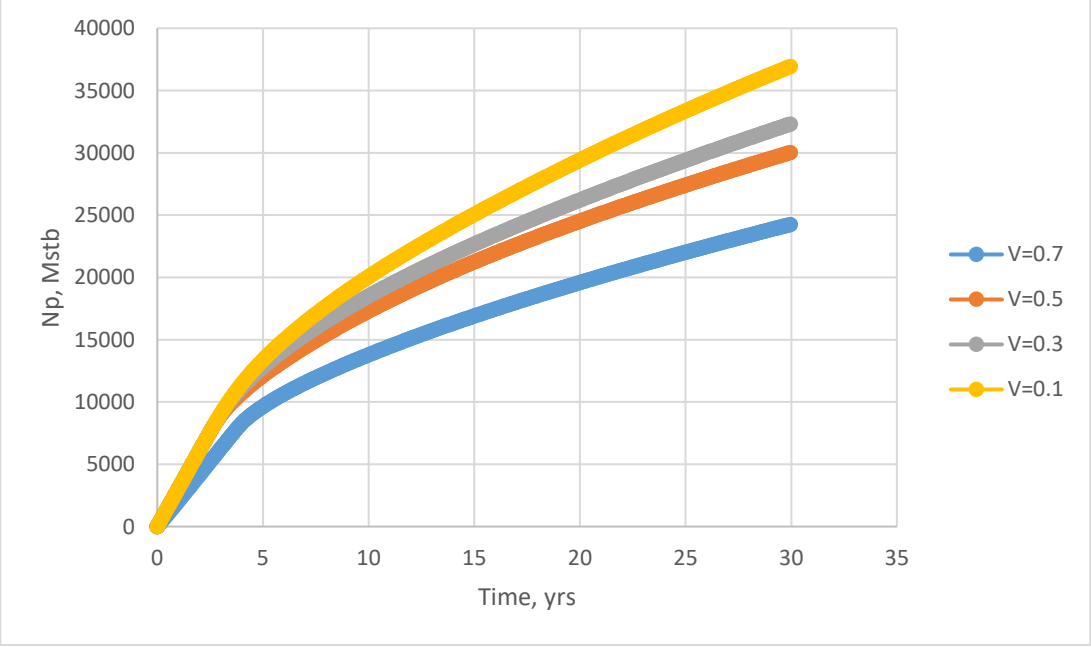

Figure 4.12: Cumulative production performance (Case 3)

4.4 Effect of permeability anisotropy ratio

Selected combination scenario:

V = 0.7, μ_w = 0.25 cP, q_i = 10,000 stb/day and k_z/k_x = 0.1 - 1

In this scenario the effects of changing the permeability anisotropy on the performance of water flood projects were studied. It can be observed in Figure 13 through 16 that changing k_z/k_x from 0 (no crossflow between layers) to one (full cross flow between layers) can have significant impacts on the various performances considered in this work. For example, in Figure 4.14 the RF dramatically increased from 5% to 45% for k_z/k_x values of 0 and 1, respectively. In addition, Figure 4.16 shows that the cumulative production increased from 5 MMstb to 35 MMstb when to total cross flow between layers. Higher water cuts and higher field pressures were observed without cross flow which is indicative of unfavorable water flood performances (Figures 4.13 and 4.15).

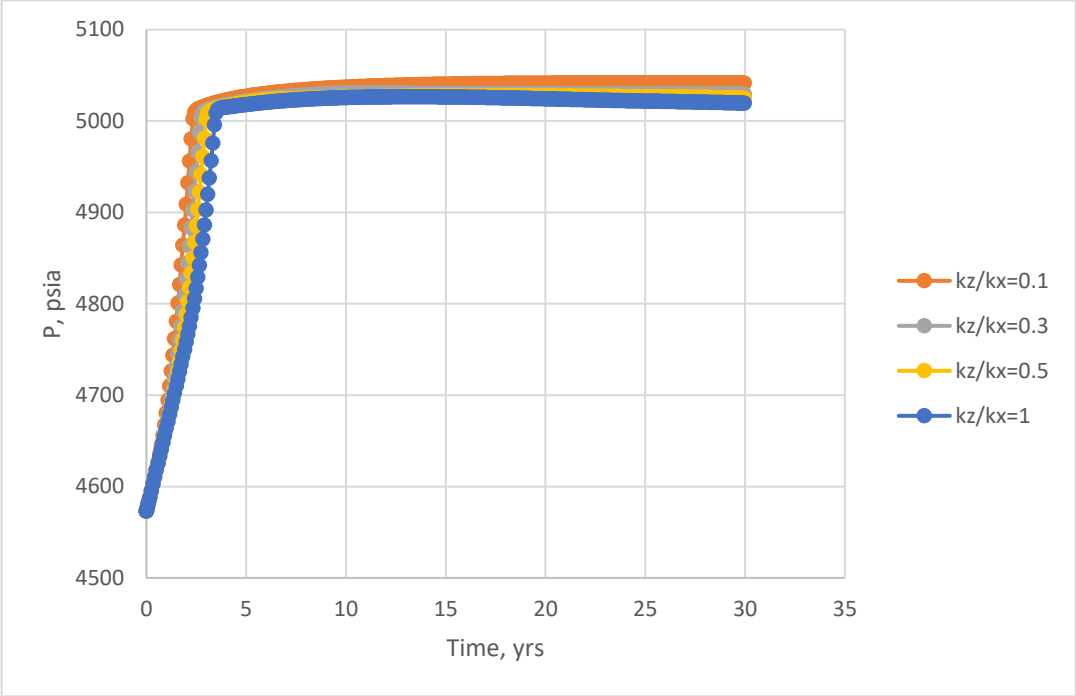

Figure 4.13: Average field pressure performance (Case 4)

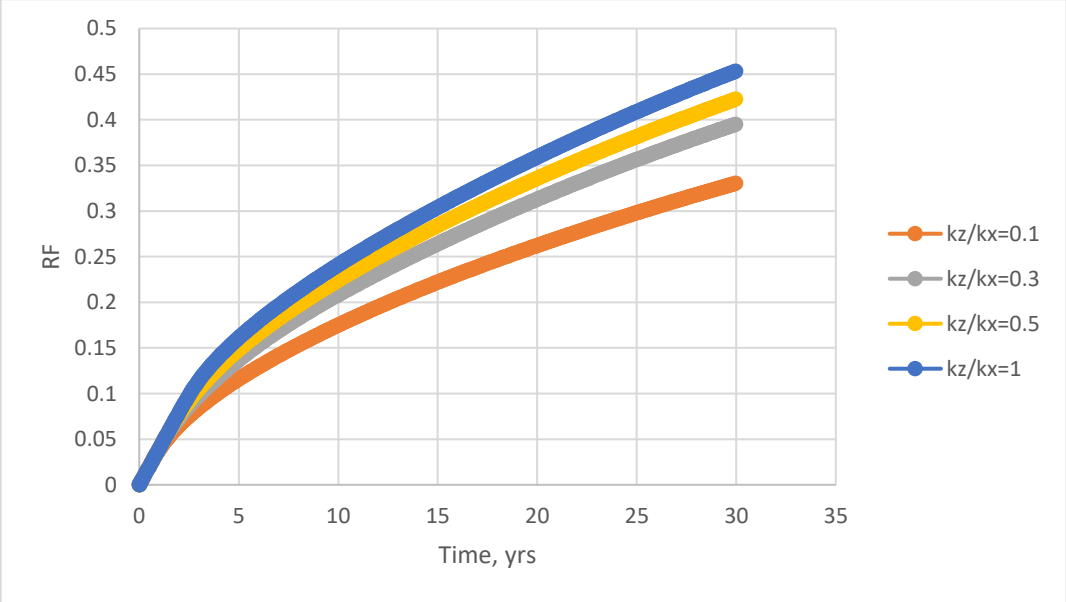

Figure 4.14: Oil recovery factor performance (Case 4)

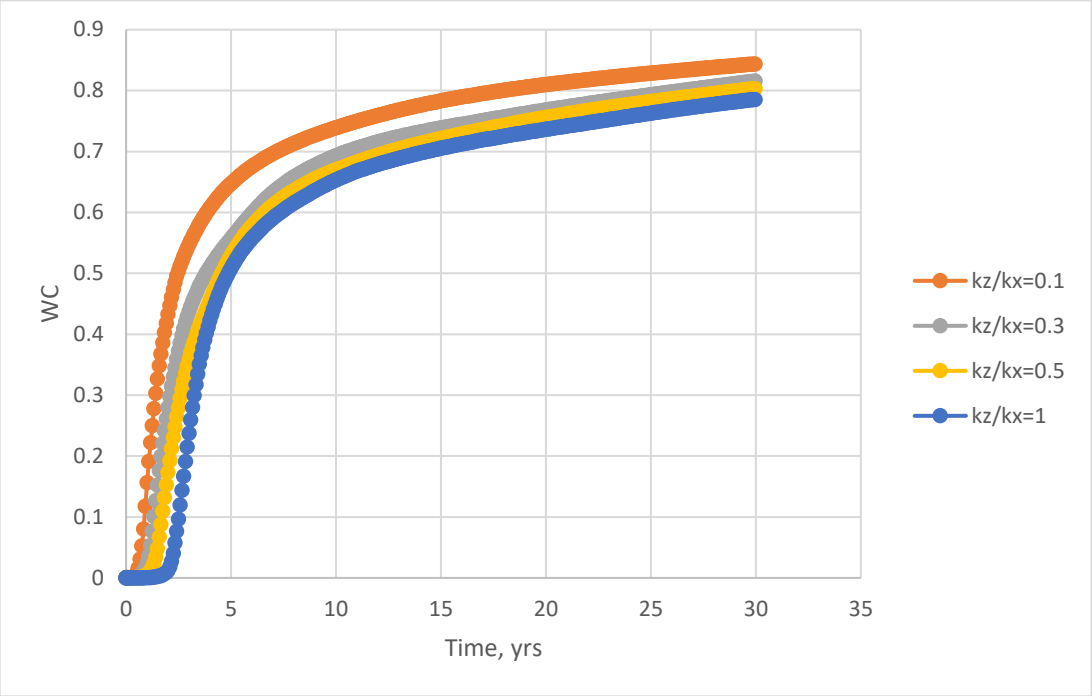

Figure 4.15: Water cut performance (Case 4)

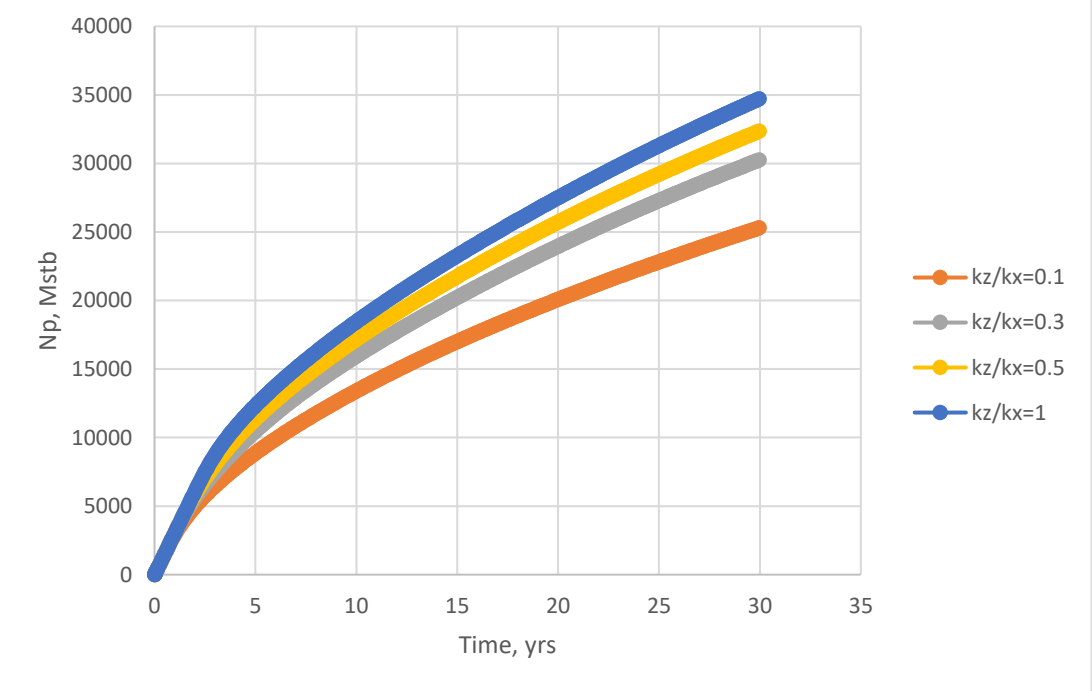

Figure 4.16: Cumulative oil production performance (Case 4)

Chapter 5: Development of New Empirical Correlations

5.1 Generating the new empirical correlation(s)

The simulation-generated data were used in the General Linear Model (GLM), provided by the Minitab Software, to develop new correlations for the oil recovery factor.

5.1.1 Predicting RF at water breakthrough time (RF_{BT}).

Based on 144 simulation-generated data (75% of the total data points) two correlations have been developed. The first correlation (Equation 5.1) encompasses the four key parameters considered in this work, and it is called the expanded form. The second correlation (Equation 5.2) and based on the GLM analysis, only considers the most significant key parameters (out four) in water flooding; this correlation represents the reduced form. The remaining 48 data points were used for testing the accuracy of the developed correlations.

$$RF_{BT} = 3.23 + 44.44(k_z/k_x) + 17.03(\mu_w) - 3.9(V) - 2.467(q_i) - 72.16(k_z/k_x)^2 - 13.1(\mu_w)^2 - 0.7(V)^2 + 0.1986(q_i)^2 + 21.4(k_z/k_x * \mu_w) - 12(k_z/k_x * V) - 0.388(k_z/k_x * q_i) - 0.3(\mu_w * V) - 1.171(\mu_w * q_i) + 1.2(V * q_i) + 31.96(k_z/k_x)^3 + 3.73(\mu_w)^3 - 6.14(k_z/k_x^2 * \mu_w) + 4.47(k_z/k_x^2 * V) + 2.23(k_z/k_x^2 * q_i) - 2.81(k_z/k_x * \mu_w^2) - 9.62(k_z/k_x * \mu_w * V) - 0.855(k_z/k_x * \mu_w * q_i) - 0.24(k_z/k_x * V^2) + 0.46(k_z/k_x * V * q_i) - 0.1779(k_z/k_x * q_i^2) - 0.25(\mu_w^2 * V) + 0.361(\mu_w^2 * q_i) + 5(\mu_w * V^2) + 0.097(\mu_w * V * q_i) + 0.0497(\mu_w * q_i^2) + 0.72(V^2 * q_i) - 0.1165(V * q_i^2) + 1.16(k_z/k_x * \mu_w * q_i * V) \quad (5.1)$$

In the new formula, RF_{BT} is the oil recovery factor at breakthrough, k_z/k_x is the anisotropy, μ_w is the water viscosity in cp, V is the permeability variation coefficient and q_i is the water injection rate in Mstb/d.

$$RF_{BT} = 3.77 + 42.28(k_z/k_x) + 11.14(\mu_w) - 2.22(V) - 2.202(q_i) - 69.3(k_z/k_x)^2 - 5.51(\mu_w)^2 + 0.1372(q_i)^2 + 11.52(k_z/k_x * \mu_w) - 6.4(k_z/k_x * V) + 3.57(\mu_w * V) - 0.1894(\mu_w * q_i) + 31.96(k_z/k_x)^3 - 6.14(k_z/k_x^2 * \mu_w) + 2.126(k_z/k_x^2 * q_i) - 0.1945(k_z/k_x * q_i^2) + 0.0843(V * q_i^2) \quad (5.2)$$

5.1.2 Predicting the RF at end of project (RF_{EOP}).

Similar developments for oil recovery factor at the end of project were attempted and the resulting correlations include an expanded form (Equation 5.3) and a reduced form (Equation 5.4).

$$RF_{EOP} = 14.09 + 14.16(k_z/k_x) - 1.41(\mu_w) - 9(V) + 1.624(q_i) - 29.39(k_z/k_x)^2 - 9.96(\mu_w)^2 + 4.93(V)^2 - 0.0848(q_i)^2 + 11.22(k_z/k_x * \mu_w) - 17.61(k_z/k_x * V) + 2.968(k_z/k_x * q_i) + 16.99(\mu_w * V) + 3.527(\mu_w * q_i) + 3.382(V * q_i) + 12.7(k_z/k_x)^3 + 4.74(\mu_w)^3 - 0.29(k_z/k_x^2 * \mu_w) + 9.4(k_z/k_x^2 * V) - 0.294(k_z/k_x^2 * q_i) - 5.82(k_z/k_x * \mu_w^2) - 0.37(k_z/k_x * \mu_w * V) - 0.122(k_z/k_x * \mu_w * q_i) + 4.89(k_z/k_x * V^2) - 0.846(k_z/k_x * V * q_i) - 0.1109(k_z/k_x * q_i^2) + 1.92(\mu_w^2 * V) - 0.453(\mu_w^2 * q_i) - 8.63(\mu_w * V^2) - 2.728(\mu_w * V * q_i) - 0.136(\mu_w * q_i^2) - 2.659(V^2 * q_i) - 0.0763(V * q_i^2) + 0.075(k_z/k_x * \mu_w * q_i * V) \quad (5.3)$$

$$RF_{EOP} =$$

$$13.862 + 13.66(k_z/k_x) - 5.399(\mu_w) - 4.56(V) + 1.713(q_i) - 29.57(k_z/k_x)^2 + 0.0848(q_i)^2 + 10.32(k_z/k_x * \mu_w) - 12.95(k_z/k_x * V) + 2.892(k_z/k_x * q_i) + 10.58(\mu_w * V) + 3.482(\mu_w * q_i) + 3.114(V * q_i) + 12.7(k_z/k_x)^3 + 9.4(k_z/k_x^2 * V) - 0.294(k_z/k_x^2 * q_i) - 5.9(k_z/k_x * \mu_w^2) - 0.8(k_z/k_x * V * q_i) - 0.1109(k_z/k_x * q_i^2) - 0.463(\mu_w^2 * q_i) - 2.692(\mu_w * V * q_i) - 0.136(\mu_w * q_i^2) - 2.413(V^2 * q_i) - 0.0763(V * q_i^2) \quad (5.4)$$

5.2 Validation of the new correlations

5.2.1 Validation of the expanded forms using 144 data points

The accuracy of the proposed correlations developed in the previous section was tested by comparing the values of RF generated by the simulator with those predicted by the new correlations. The results of these comparisons are illustrated in Figure 5.1 and Figure 5.2.

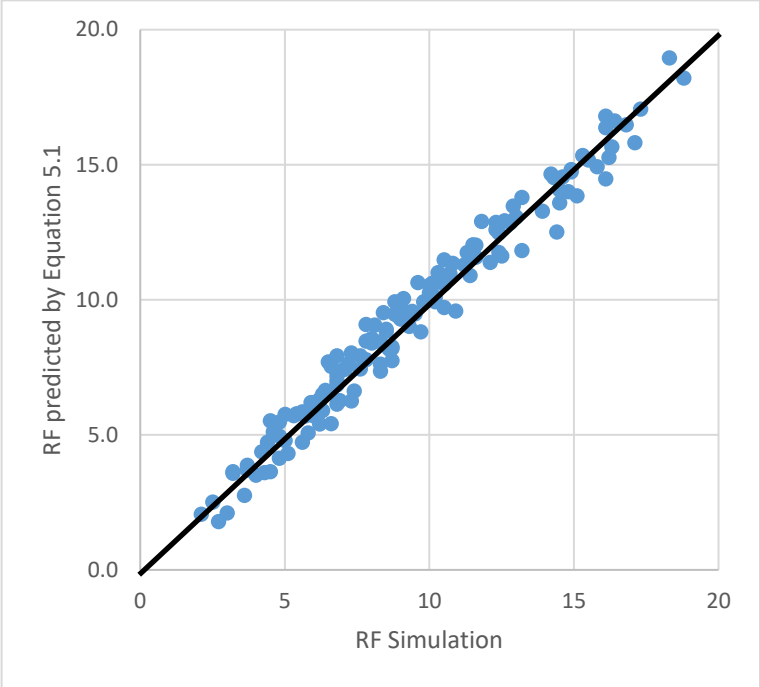

Figure 5.1: Comparison between RF_{BT} predicted by Equation 5.1 and generated by the simulator

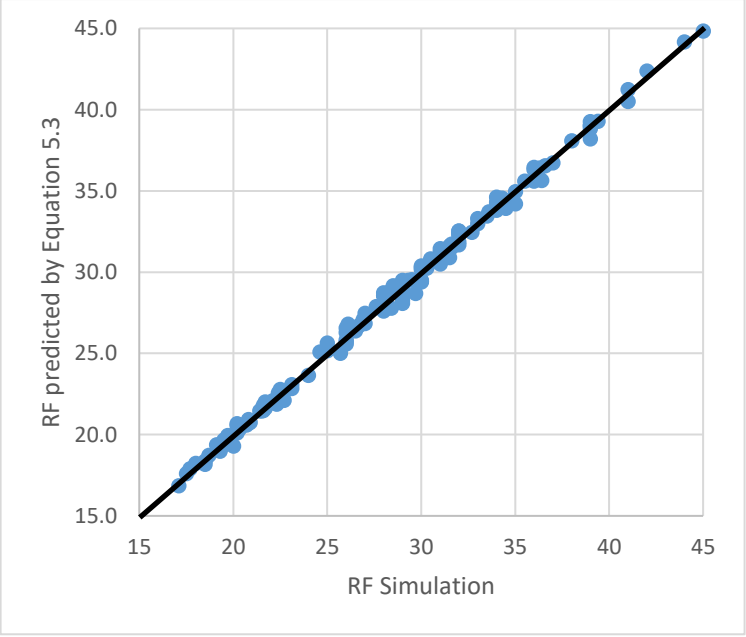

Figure 5.2: Comparison between RF_{EOP} predicted by Equation 5.3 and generated by the simulator

5.2.2 Validation of the reduced forms using 144 data points

Similar comparisons were performed for testing the reduced forms expressed in Equation 5.2 and 5.4 and the results are shown in Figure 5.3 and 5.4. The 45-degree line in Figure 5.1 through 5.8 represents the perfect match location between the simulated and predicted RF values.

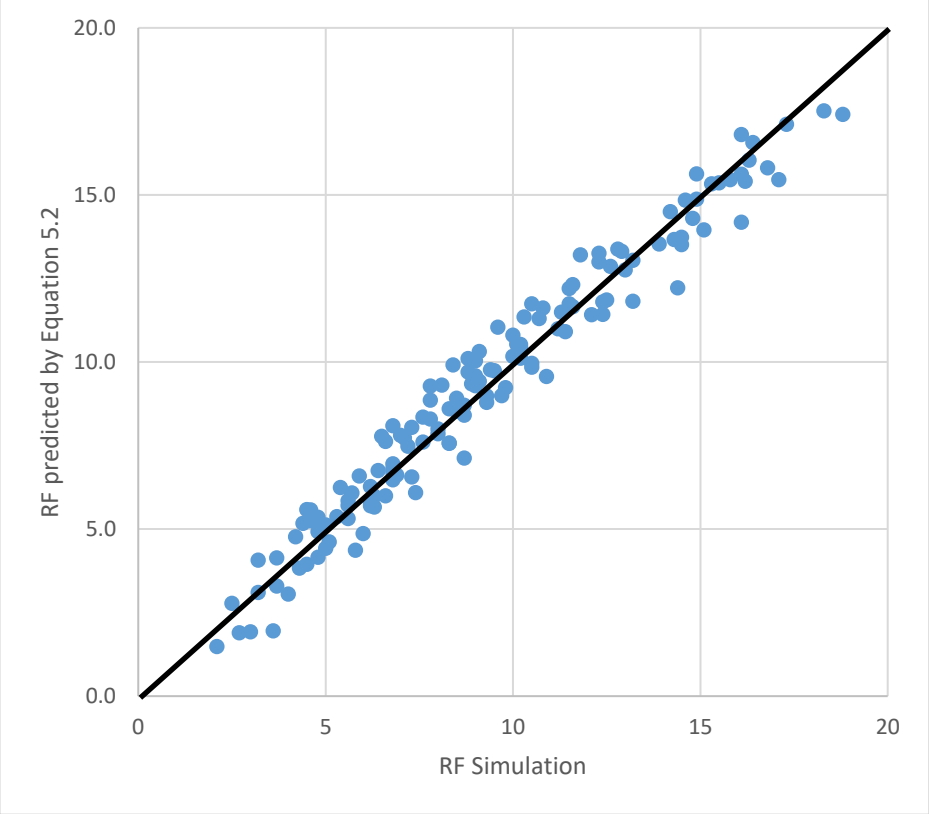

Figure 5.3: Comparison between RF_{BT} predicted by Equation 5.2 and generated by the simulator

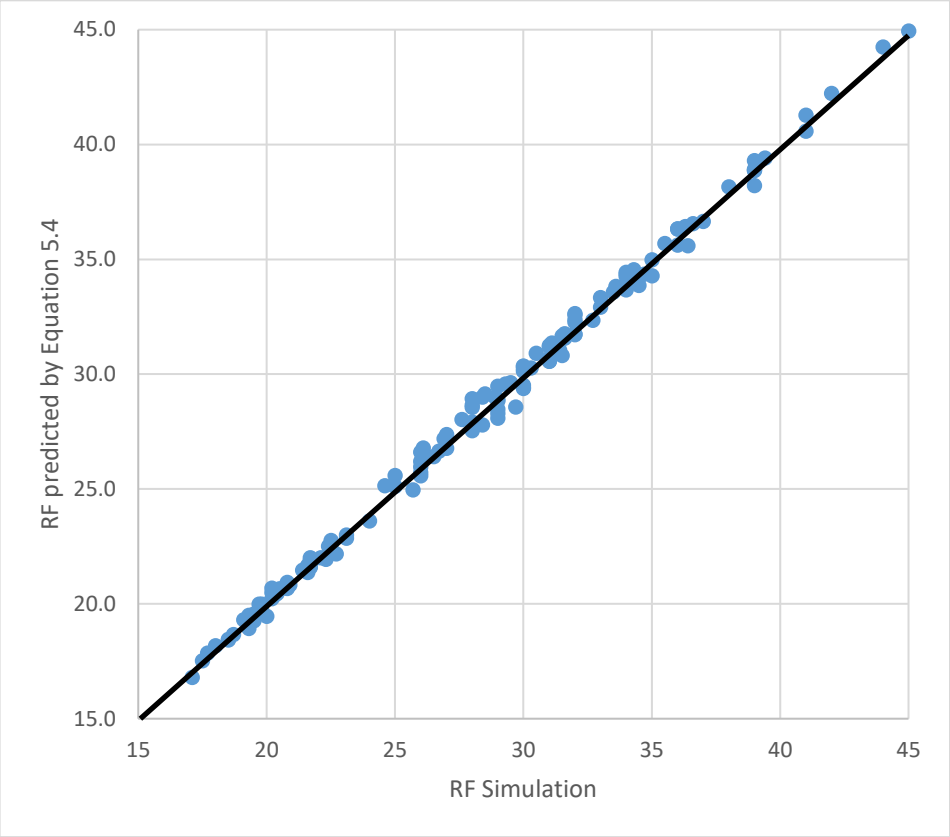

Figure 5.4: Comparison between RF_{EOP} predicted by Equation 5.4 and generated by the simulator

5.2.3 Validation of the expanded forms using the remaining 48 data points

The second part of the validation was accomplished by considering the remaining 48 data of the total 192 data points. These 48 data points represent data which have been used in the development of the new correlations. Equation 5.1 was applied to calculate the RF_{BT} for the 48 data points and the results were compared with the simulation-generated results. The results of this comparison are shown in Figure 5.5.

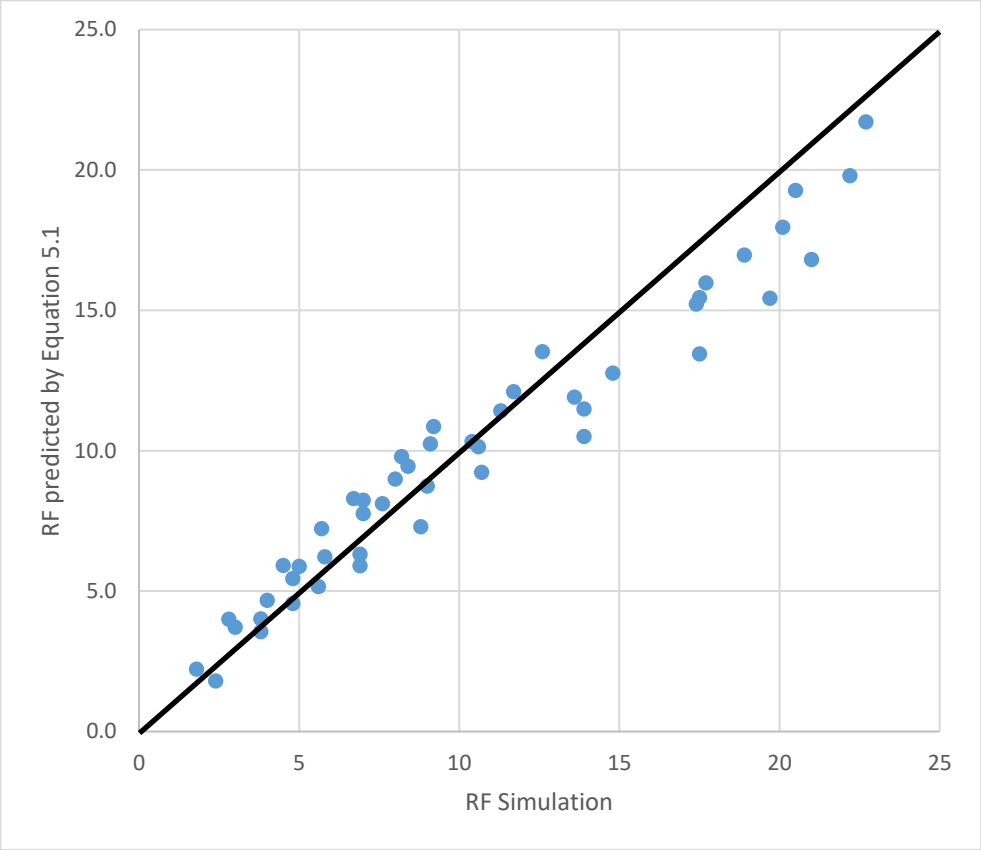

Figure 5.5: Comparison between predicted RF_{BT} values by Equation 5.1 and by simulator

A similar comparison between RF_{EOP} predicted by Equation 5.3 and by simulation is illustrated in Figure 5.6.

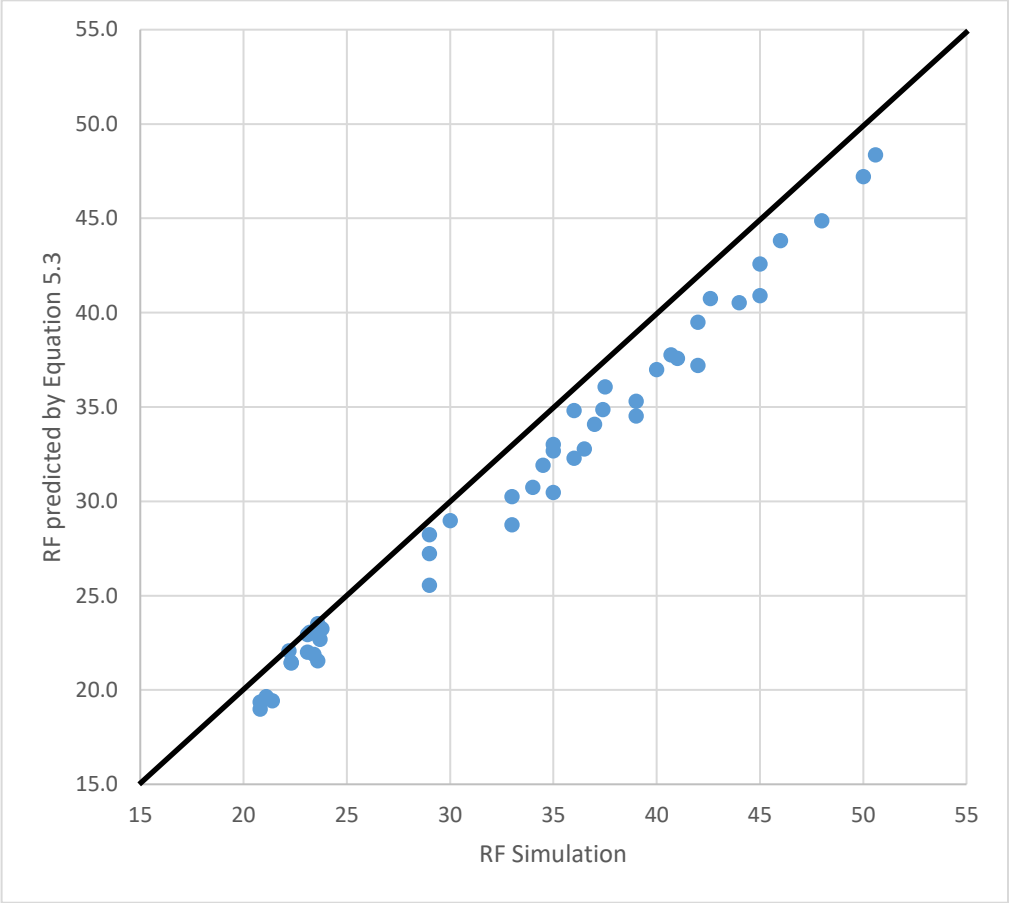

Figure 5.6: Comparison between predicted by Equation 5.3 and simulated values of RF_{EOP}

In addition, the reduced forms, Equation 5.2 and Equation 5.4, have been applied for the 48 data points and the results of the comparison are shown in Figure 5.7 and Figure 5.8

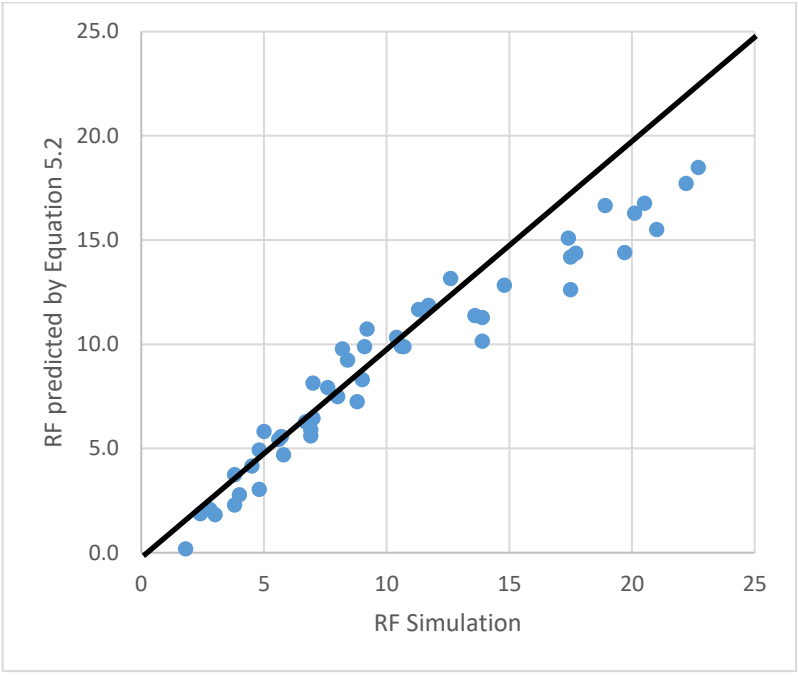

Figure 5.7: Comparison between predicted by Equation 5.2 and simulated values of RF_{BT}

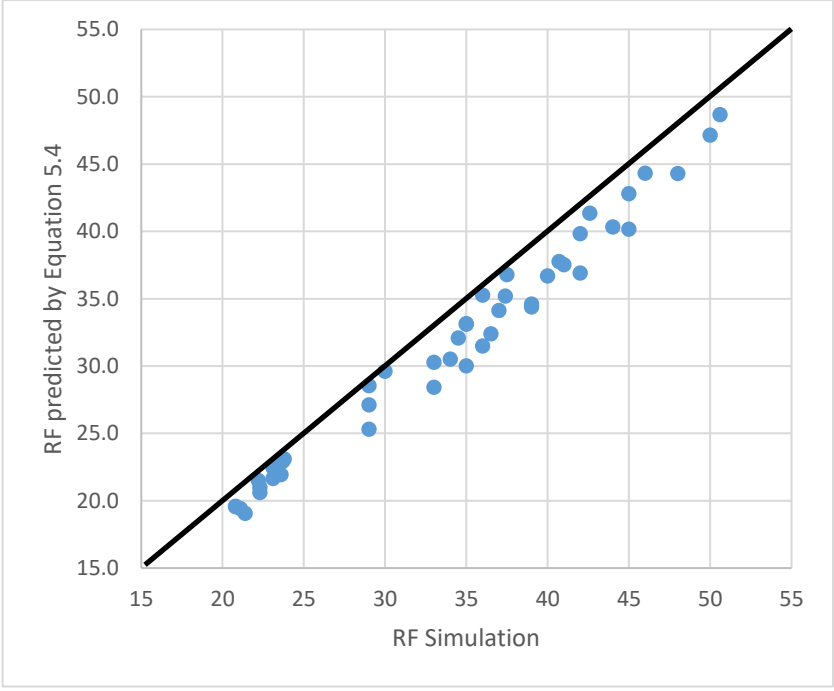

Figure 5.8: Comparison of predicted values by Equation 5.4 and simulated values of RF_{EOP}

The results of calculations of the absolute percent difference (APCD) for the individual combination scenarios of RF_{BT} and RF_{EOP} are listed in Table B.1 through Table B.4 of appendix B. The average absolute percent difference (AAPCD) was then calculated for each case and the summary of the results are shown in Table 5.1.

Table 5.1: Results of calculations of AAPCD for various cases investigated

Case	RF_{BT} by Equation (5.1)	RF_{BT} by Equation (5.2)	RF_{EOP} by Equation (5.3)	RF_{EOP} by Equation (5.4)
144 data points	6.90	8.30	1.02	1.04
48 data points	14.00	16.90	6.50	6.70

5.3 Validation of the new correlations using field data

In this section, the new correlations were validated using Field A data listed in Table 5.2 [13]. The recovery factor was obtained with Visual Basic for Applications (VBA) program and for this case yields RF_{EOP} of 0.396. The value of RF_{BT} is not available for this field and thus, the only possible comparison was between the predicted values of RF_{EOP} by various methods and the field value.

Table 5.2: Field case data

Reservoir name	Field A
Oil viscosity, cp	1.2
Water viscosity, cp	0.9
Corey exponent for oil (n_o)	3.017
Corey exponent for water (n_w)	1.8045
End point-relative permeability to oil (k_{roe})	0.96865
End point-relative permeability to water (k_{rwe})	0.551
Residual oil saturation (S_{or})	0.23
Connate water saturation (S_{wc})	0.38
Dykstra Parson Coefficient (V)	0.8
Water wet=1 or oil wet=2	1.0
Estimated max operational WOR	26.3
Permeability anisotropy ratio (k_z/k_x)	1.0
Injection rate, stb/d	8,000

The value of RF_{EOP} was estimated by three empirical correlations, namely, Guthrie-Greenberger correlation, Equation (2.1), API statistical study, Equation (2.2) and the proposed new correlations, Equation 5.3 and Equation (5.4). The predicted values of RF_{EOP} were then compared with the field observation and the absolute per cent difference for each method was calculated. The results of these calculations are illustrated in Table 5.3.

Table 5.3: Predicted values of RF_{EOP} versus field value

Correlation	Field Case	Guthrie-Greenberger Method (Equation 2.1)	API Statistical Study (Equation 2.2)	New Correlation (Equation 5.3)	New Correlation (Equation 5.4)
RF_{EOP}	0.396	0.399	0.472	0.308	0.309
APCD	-	0.758	19.2	22.9	22.7

Chapter 6: Discussion of Results

6.1 Discussion of simulation results (Eclipse)

The generated relative permeability curves generated by Corey's correlations (Figure 3.2), intersect at water saturation of 0.65 which is indicative of a water-wet system. The reservoir is assumed to consist of ten layers which have different permeabilities and that there is a significant variation in the values of permeability of these layers across the reservoir thickness. This variation is illustrated in Table 3.2 which shows that as the permeability variation coefficient (*V*) increases from 0.1 to 0.7, the reservoir becomes more heterogeneous. The permeabilities of the ten layers were arranged in a descending order which indicative of permeability coarsing upward across the reservoir. Such permeability arrangement scenario would promote gravity effects during the process of water flooding provided that cross flow exists between layers.

The water-oil mobility ratio dictates the shape of water front, and thus, the in-situ water saturation profile with injection time during the flooding process. The mobility ratio has a great influence on water flood efficiency at and beyond water breakthrough as shown in Figures 4.1 through 4.4. Oil reservoirs with favorable mobility ratio ($M \leq 1.0$) yield higher oil recovery (RF) as compared to unfavorable mobility ratio ($M > 1.0$) as indicated by 12% increase of oil recovery shown in Figure 4.2. Favorable mobility ratios are usually associated with low oil viscosity.

The effect of the injection rate on the RF can be realized in Figures 4.5 through 4.8. As the water injection rate is increased from 2,000 stb/d to 10,000 stb/d, the

performance of water flooding operation improved. There is a dramatic increase of 30% in the value of RF as shown in Figure 4.6. Faster reservoir pressure maintenance is usually associated with higher water injection rates and thus, better water flooding performance in terms of oil production. The negative aspects of higher water injection rates, however, include faster water breakthrough and higher water cuts with time. With high injection rate, water will advance fast enough in the high permeability layers to render gravity effects ineffective.

Oil recovery factor highly depends on the coefficient of permeability variation [10]. From the results, the effects of permeability variation on oil recovery factor at breakthrough and at end of the project show that larger permeability variation results in poorer oil recovery with different cases of mobility ratios. The dependence of RF on V is confirmed in Figures 4.9 through 4.12 where the value of V was varied between 0.1 and 0.7. Figure 4.10 shows a 13% increase in the RF when the reservoir is homogeneous rather than heterogeneous reservoirs. Also, the results of cumulative production confirm additional 14 MMstb of oil with V of 0.1.

The effect of permeability anisotropy ratio was analyzed at breakthrough and end of water flood project for very favorable and unfavorable mobility ratios. Increased crossflow, as indicated by increased k_z/k_x ratio, has been found to improve water flood project performance as shown in Figure 4.13 through 4.16. It can be observed that the recovery factor increases by 10% when changing k_z/k_x ratio from 0.1 to 1.0 (Figure 4.14). Moreover, the cumulative production is improved by 10 MMstb when the ratio is changed from 0.1-1 (Figure 4.16) which, confirms the improvement in the performance. Improved overall performance of water flooding process with crossflow is attributed to the net effect

of gravity and rate of water injection. At the lower injection rates (2,000 and 5,000 bpd), gravity can be very effective in controlling the shape of the water front such that a piston-like displacement is most likely achieved. Such displacement mechanism will result in a more efficient water flood process even with unfavorable mobility ratio. Furthermore, the negative aspect of having no crossflow is reaching the maximum of water production faster than with cross flow case which is not favorable for water flooding projects [11].

6.2 Discussion of validity of proposed correlations (Minitab results)

Minitab was used to generate the new correlations for predicting RF_{BT} and RF_{EOP}. The program can also identify the relative importance of the four key parameters which were included in the developed correlations. Using General Linear Model (GLM), the water injection rate has been found as the most effective parameter and that water viscosity as the least effective parameter as far as the recovery factor is concerned.

The accuracy of the new proposed correlations (Equation 5.1 for predicting RF_{BT}, and Equation 5.3 for predicting RF_{EOP}) which include all four key parameters, were tested as follows: (1) against 144 simulation-generated data points used in their development, (2) against the remaining 48 simulation-generated data points not included in the development of the new correlations, and (3) against a real field case data. Similarly, the reduced forms of the new correlations (Equation 5.2 for predicting RF_{BT} and Equation 5.4 for predicting RF_{EOP}), were tested as described above. The results of comparisons of (1) and (2) are shown in Figure 5.1 through 5.8. From these plots, it is observed that the data are nearly identical and falls on the fitted line for case 1 of validation. On the other hand, there is a small deviation between the predicted values and simulation results as can be

noticed through Figures 5.5 through 5.8 and that is for case 2. This is representative of the relative error produced using each validation method and it's with an acceptable range. In addition, the AAPCD for all 144 values of RF_{BT} and RF_{EOP} were calculated and the results are presented in Table B.1 and B.2 of Appendix B, respectively. Similar results of calculations of AAPCD for the remaining 48 data points are presented in Table B.3 and B.4 of Appendix B, respectively. A summary of the AAPCD results is shown in Table 5.1. For both validity cases considered in this study, and as expected, it can be observed that the proposed expanded forms yield more accurate results than the proposed reduced forms. For the 144 data points case an AAPCD as low as 1.02 has been obtained for predicting RF_{EOP} with Equation 5.3.

The reliability of the proposed correlations was further tested using published data of a water flood project with data listed in Table 5.2 [13]. The value of field RF_{EOP} was compared with RF_{EOP} predicted by three methods, namely, Guthrie-Greenberger method, API Statistical Study, and the proposed correlations. The results of this comparison are presented in Table 5.3. These results are not indicative of the superiority of any of the methods considered in this study simply because a single field data point has been used. However, the high APCD values of the proposed correlations are comparable to those of the API method. The fact that the permeability variation coefficient for this field data (V = 0.8) is higher than the maximum value considered in the development of the proposed correlations (V = 0.7) may explain the relatively high APCD values in Table 5.3. Additional field data are necessary to examine the proposed correlations.

6.3 Discussion of limitations of the proposed correlations

The new empirical correlations developed in this study are based on four key parameters believed to impact the overall performance of water flood operations. Therefore, the proposed correlations will depend very much on the availability of these key parameters, which puts a limitation on their application. Moreover, the selected four parameters may not be enough to evaluate the effectiveness of the water flood performance in terms of oil recovery and water cut profiles. Other reservoir characteristics, such wettability preference, initial free gas saturation, and dip angle could very much affect the accuracy of the proposed correlations.

The proposed empirical correlations were developed for specific ranges of key parameters as shown in Table 3.6. Therefore, the application of Equations. 5.1 through 5.4 outside these ranges, and specifically for V and q_i, may not yield accurate RF_{BT} and RF_{EOP}.

Chapter 7: Conclusion and Recommendation

7.1 Conclusion

Based on the results of this study, the following conclusions can be drawn.

- Two sets of new empirical correlations have been developed to predict the performance of a 5-spot water flood in a stratified reservoir. These correlations encompass four key parameters believed to significantly affect the oil recovery factors in water flood operations. These key parameters include water injection rate, water viscosity, permeability anisotropy, and reservoir heterogeneity.
- When tested against 144 simulation-generated data points used in their development, the expanded forms of the new correlations have been found to give reliable estimates of RF_{BT} and RF_{EOP} with AAPCD of 6.9 and 1.02, respectively. The reduced forms were found to yield a slightly higher AAPCD for the same data set.
- When tested against 48 simulation-generated data points representing ranges of key parameters outside the ones used their development, the expanded forms of the new correlations have been found to give good estimates of RF_{BT} and RF_{EOP} with AAPCD of 6.5 and 14, respectively.
- The new correlations have been found to give more accurate estimates of RF_{EOP} than for RF_{BT}. The highest RF_{EOP} of 50.6% was achieved for a combination scenario defined by: q_i = 10,000 bpd, μ_w = 1.0 cp, k_z/k_x = 1.0, and V = 0.1.
- When tested against two published empirical correlations using a single field data point, the proposed correlations were found to give relatively high APCD. The

failure of the proposed correlations to yield accurate results in this case may be attributed to a value of V that is outside the range of this parameter as presented in Table 3.6.

- It is believed that the results and conclusions of this work present a valuable addition to the literature.
- Provided reliable ingredients were available, the new correlations can be used to get quick and reliable estimates of RF_{BT} and RF_{EOP}.

7.2 Recommended measures to improve the accuracy

Based on the limitations addressed in section 6.3, the following can be recommended.

- Including the effects of free gas saturation, angle of dip, wettability preference indicator in the proposed correlation would certainly improve their accuracy.
- Benchmarking with other analytical methods and simulation results using more field data is necessary.
- The total number of simulation-generated data point used in the development of the proposed correlations can be increased by considering additional combination scenarios of key parameters.

References

1- Petrowiki. (2018). Water flooding. Retrieved (5/May/ 2020) from www.petrowiki.org/waterflooding.

2- Ahmed, T. (2002). Reservoir Engineering Handbook. 2nd Edition. Houston, Texas: Gulf Professional Publishing.

3- Wikipedia. (2020). List of oil and gas fields of the North Sea. Retrieved (5/May/ 2020) from https://en.wikipedia.org/wiki/List_of_oil_and_gas_fields_of_the_North_Sea

4- Lyons, W., and Plisga, G. (2004). Standard Handbook of Petroleum and Natural Gas Engineering, P.E., Gulf Professional Publishing.

5- Oseh1, J. O., and Omotara O. O. (2014). Recovery Factor Model Study in the Niger Delta Oil Reservoir for Water Drive Mechanism. Afc Babalola University.

6- Khan, A. (1971). An Empirical Approach to Waterflood Predictions. Journal of Petroleum Technology. 23(05), 565–573. doi: 10.2118/2931-pa.

7- Barbieri, R. R. (1996). Statistical Secondary Recovery Model. SPE Advanced Technology Series. 4(01), 44–52. doi: 10.2118/26978-pa.

8- Petrofaq. (2014). Eclipse input data. Retrieved (5/May/ 2020) from http://petrofaq.org/wiki/Eclipse_Input_Data.

9- Tompang, R., and Kelkar, B. (1988). Prediction of Waterflood Performance in Stratified Reservoirs. Permian Basin Oil and Gas Recovery Conference. doi: 10.2118/17289-ms

10- El-Khatib, N. (April 2003). Effect of Gravity on Waterflooding Performance of Stratified Reservoirs. Paper SPE 81465 presented at the SPE 13th Middle East Oil Show and Exhibition, Bahrain.

11- El-Khatib, N. (1985). The Effect of Crossflow on Waterflooding of Stratified Reservoirs. SPE Journal of Reservoir Engineering. 25:291-302. Doi: 10.2118/11495-PA

12- El-Khatib, N. (1999). Waterflooding Performance of Communicating Stratified Reservoirs with Log-Normal Permeability Distribution. SPE Journal of Reservoir Evaluation and Engineering. 2(6), 542-549.

13- Espinel, A. L. (Dec. 2010). Generalized Correlation to Estimate Oil Recovery and Pore Volumes Injected in Waterflooding Projects, Ph.D. dissertation, Texas A and M University, College Station, Texas.

14- Arps, J. J., and Ertekin, T. (1967). Statistical Analysis of Crude Oil Recovery and Recovery Efficiency, Bulletin D14, American Petroleum Institute, Washington D.C.

15- Mahmoud, A. A., Elkatatny, S., Chen, W., and Abdulraheem, A. (2019). Estimation of Oil Recovery Factor for Water Drive Sandy Reservoirs through Applications of Artificial Intelligence. Energies. 12(19), 3671. doi:10.3390/en12193671

16- Balhasan S., and Jumaa, M. (2017). Development of a Correlation to Predict Water-Flooding Performance of Sandstone Reservoirs Based on Reservoir Fluid Properties. International Journal of Applied Engineering Research ISSN. 12(10), 2586-2597. Research India Publications. http://www.ripublication.com.

17- Gulstad, R. L. (1995). The Determination of Hydrocarbon Reservoir Recovery Factors by Using Modern Multiple Linear Regression Techniques. Master's Thesis, Texas A and M University, College Station, TX, USA.

Appendices

Appendix A

Detailed Results of simulation and Minitab

Table A.1: Results of Eclipse

kz/kx	μ_w*(cP)*	*V*	q_i*(Mstb/d)*	RF_{BT}	RF_{EOP}
0.1	0.25	0.1	2	6.9	21.4
0.1	0.25	0.1	5	2.4	29
0.1	0.25	0.1	10	1.8	33
0.3	0.25	0.1	2	13.9	22.3
0.3	0.25	0.1	5	5	33
0.3	0.25	0.1	10	2.8	39
0.5	0.25	0.1	2	13.6	22.2
0.5	0.25	0.1	5	8.8	35
0.5	0.25	0.1	10	3.8	42
1	0.25	0.1	2	13.9	22.3
1	0.25	0.1	5	10.7	36
1	0.25	0.1	10	6.9	45
0.1	0.5	0.1	2	7.6	21.1
0.1	0.5	0.1	5	3.8	29
0.1	0.5	0.1	10	3	35
0.3	0.5	0.1	2	17.5	23.1
0.3	0.5	0.1	5	7	34
0.3	0.5	0.1	10	4.5	41

0.5	0.5	0.1	2	17.5	23.1
0.5	0.5	0.1	5	10.6	36.5
0.5	0.5	0.1	10	5.8	44
1	0.5	0.1	2	17.7	23.2
1	0.5	0.1	5	14.8	39
1	0.5	0.1	10	9	48
0.1	0.75	0.1	2	8.4	20.8
0.1	0.75	0.1	5	4.8	29
0.1	0.75	0.1	10	4	36
0.3	0.75	0.1	2	19.7	23.4
0.3	0.75	0.1	5	8.2	34.5
0.3	0.75	0.1	10	5.7	42
0.5	0.75	0.1	2	20.1	23.5
0.5	0.75	0.1	5	11.7	37
0.5	0.75	0.1	10	7	45
1	0.75	0.1	2	20.5	23.6
1	0.75	0.1	5	17.4	40
1	0.75	0.1	10	10.4	50
0.1	1	0.1	2	9.1	20.8
0.1	1	0.1	5	5.6	30
0.1	1	0.1	10	4.8	37.5
0.3	1	0.1	2	21	23.6
0.3	1	0.1	5	9.2	35
0.3	1	0.1	10	6.7	42.6

0.5	1	0.1	2	22.2	23.7
0.5	1	0.1	5	12.6	37.4
0.5	1	0.1	10	8	46
1	1	0.1	2	22.7	23.8
1	1	0.1	5	18.9	40.7
1	1	0.1	10	11.3	50.6
0.1	0.25	0.3	2	4.6	19.3
0.1	0.25	0.3	5	2.7	26
0.1	0.25	0.3	10	2.1	30.5
0.3	0.25	0.3	2	10.9	20.4
0.3	0.25	0.3	5	4.5	29
0.3	0.25	0.3	10	3.2	34
0.5	0.25	0.3	2	10.1	20.2
0.5	0.25	0.3	5	6.4	30
0.5	0.25	0.3	10	4	36
1	0.25	0.3	2	9.4	19.8
1	0.25	0.3	5	8.6	31
1	0.25	0.3	10	5.6	39
0.1	0.5	0.3	2	6.5	19.5
0.1	0.5	0.3	5	4.5	27
0.1	0.5	0.3	10	3.7	33
0.3	0.5	0.3	2	14.4	21.6
0.3	0.5	0.3	5	6.8	30
0.3	0.5	0.3	10	5.3	37

0.5	0.5	0.3	2	14.5	21.7
0.5	0.5	0.3	5	9	32
0.5	0.5	0.3	10	6.3	39
1	0.5	0.3	2	13.2	21.6
1	0.5	0.3	5	12.5	34
1	0.5	0.3	10	8.3	42
0.1	0.75	0.3	2	7.8	19.8
0.1	0.75	0.3	5	5.6	28
0.1	0.75	0.3	10	5	35
0.3	0.75	0.3	2	16.1	22.3
0.3	0.75	0.3	5	8.4	31.5
0.3	0.75	0.3	10	6.8	38
0.5	0.75	0.3	2	16.8	22.5
0.5	0.75	0.3	5	10.5	33
0.5	0.75	0.3	10	8.3	41
1	0.75	0.3	2	16.1	22.5
1	0.75	0.3	5	14.8	36
1	0.75	0.3	10	10	44
0.1	1	0.3	2	8.8	20.2
0.1	1	0.3	5	6.6	29.3
0.1	1	0.3	10	6	35
0.3	1	0.3	2	17.1	22.7
0.3	1	0.3	5	9.6	32
0.3	1	0.3	10	8	39

0.5	1	0.3	2	18.8	23.1
0.5	1	0.3	5	11.8	34
0.5	1	0.3	10	9.3	41
1	1	0.3	2	18.3	23.1
1	1	0.3	5	16.3	36.6
1	1	0.3	10	11.6	45
0.1	0.25	0.5	2	4.6	18.5
0.1	0.25	0.5	5	3	24.6
0.1	0.25	0.5	10	2.5	29.5
0.3	0.25	0.5	2	9.7	19.3
0.3	0.25	0.5	5	4.8	26.9
0.3	0.25	0.5	10	3.7	32
0.5	0.25	0.5	2	8.8	20
0.5	0.25	0.5	5	6.2	27.6
0.5	0.25	0.5	10	4.3	33.6
1	0.25	0.5	2	7.8	18.5
1	0.25	0.5	5	7.6	28
1	0.25	0.5	10	5.6	35.5
0.1	0.5	0.5	2	6.6	19.1
0.1	0.5	0.5	5	4.8	26.7
0.1	0.5	0.5	10	4.2	31.5
0.3	0.5	0.5	2	13.2	20.8
0.3	0.5	0.5	5	7.3	28.9
0.3	0.5	0.5	10	5.9	34.5

0.5	0.5	0.5	2	12.6	20.8
0.5	0.5	0.5	5	9	30
0.5	0.5	0.5	10	6.9	36.4
1	0.5	0.5	2	11.5	20.5
1	0.5	0.5	5	11.4	31.6
1	0.5	0.5	10	8.5	39
0.1	0.75	0.5	2	8.1	19.7
0.1	0.75	0.5	5	6.2	28.4
0.1	0.75	0.5	10	5.7	31.1
0.3	0.75	0.5	2	15.1	21.5
0.3	0.75	0.5	5	9	30.3
0.3	0.75	0.5	10	7.6	34.3
0.5	0.75	0.5	2	15.3	21.8
0.5	0.75	0.5	5	10.8	31.6
0.5	0.75	0.5	10	8.7	36.3
1	0.75	0.5	2	14.2	21.7
1	0.75	0.5	5	13.9	33.5
1	0.75	0.5	10	10.7	39.4
0.1	1	0.5	2	9.1	20.2
0.1	1	0.5	5	7.3	29.7
0.1	1	0.5	10	6.8	31
0.3	1	0.5	2	16.2	22.1
0.3	1	0.5	5	10.3	31.4
0.3	1	0.5	10	9.1	34

0.5	1	0.5	2	17.3	22.5
0.5	1	0.5	5	12.3	32.7
0.5	1	0.5	10	10.2	36
1	1	0.5	2	16.4	22.4
1	1	0.5	5	15.8	34.7
1	1	0.5	10	12.3	39
0.1	0.25	0.7	2	4.8	17.5
0.1	0.25	0.7	5	3.6	24
0.1	0.25	0.7	10	3.2	26.5
0.3	0.25	0.7	2	8.7	18
0.3	0.25	0.7	5	5	25
0.3	0.25	0.7	10	4.4	29
0.5	0.25	0.7	2	7.8	17.7
0.5	0.25	0.7	5	6.2	25
0.5	0.25	0.7	10	5.1	30
1	0.25	0.7	2	6.8	17.1
1	0.25	0.7	5	6.8	26
1	0.25	0.7	10	6.3	31
0.1	0.5	0.7	2	7.2	18.7
0.1	0.5	0.7	5	5.8	25.7
0.1	0.5	0.7	10	5.4	26.1
0.3	0.5	0.7	2	12.1	19.7
0.3	0.5	0.7	5	8	27
0.3	0.5	0.7	10	7	28.5

0.5	0.5	0.7	2	11.5	19.7
0.5	0.5	0.7	5	9.3	28
0.5	0.5	0.7	10	8.3	30
1	0.5	0.7	2	10.2	19.5
1	0.5	0.7	5	10.5	29
1	0.5	0.7	10	9.8	32
0.1	0.75	0.7	2	8.9	19.6
0.1	0.75	0.7	5	7.4	26
0.1	0.75	0.7	10	7.1	26.1
0.3	0.75	0.7	2	14.5	20.7
0.3	0.75	0.7	5	10	28
0.3	0.75	0.7	10	9.5	28.4
0.5	0.75	0.7	2	14.6	20.9
0.5	0.75	0.7	5	11.3	29
0.5	0.75	0.7	10	10.5	30
1	0.75	0.7	2	12.8	20.8
1	0.75	0.7	5	13	31
1	0.75	0.7	10	12.4	32
0.1	1	0.7	2	10.2	20.3
0.1	1	0.7	5	8.7	26
0.1	1	0.7	10	8.5	26
0.3	1	0.7	2	15.5	21.4
0.3	1	0.7	5	11.6	28
0.3	1	0.7	10	11.2	29

0.5	1	0.7	2	16.1	21.7
0.5	1	0.7	5	12.9	29
0.5	1	0.7	10	12.4	30
1	1	0.7	2	14.9	21.7
1	1	0.7	5	14.9	31
1	1	0.7	10	14.3	32

Results of Minitab for RF_{BT}

Table A.2: Significance of parameters

Analysis of Variance

Source	DF	Seq SS	Contribution	Adj SS	Adj MS	F-Value	P-Value
Kz/Kx	1	873.89	22.27%	93.033	93.033	103.32	0.000
μw	1	953.41	24.30%	31.514	31.514	35.00	0.000
V	1	18.56	0.47%	56.650	56.650	62.91	0.000
Qi	1	1002.93	25.56%	234.966	234.966	260.95	0.000
Kz/Kx*Kz/Kx	1	209.58	5.34%	50.857	50.857	56.48	0.000
μw*μw	1	21.13	0.54%	21.134	21.134	23.47	0.000
V*V	1	26.93	0.69%	18.829	18.829	20.91	0.000
Qi*Qi	1	111.67	2.85%	151.254	151.254	167.98	0.000
Kz/Kx*μw	1	38.96	0.99%	17.161	17.161	19.06	0.000
Kz/Kx*V	1	79.40	2.02%	79.405	79.405	88.19	0.000
μw*V	1	10.73	0.27%	10.726	10.726	11.91	0.001
V*Qi	1	205.46	5.24%	38.299	38.299	42.53	0.000
Kz/Kx*Kz/Kx*Kz/Kx	1	26.17	0.67%	26.175	26.175	29.07	0.000
Kz/Kx*Kz/Kx*μw	1	4.38	0.11%	4.379	4.379	4.86	0.029
Kz/Kx*Kz/Kx*Qi	1	1.25	0.03%	156.338	156.338	173.63	0.000
Kz/Kx*μw*Qi	1	40.63	1.04%	14.626	14.626	16.24	0.000
Kz/Kx*Qi*Qi	1	124.82	3.18%	124.816	124.816	138.62	0.000
V*V*Qi	1	4.00	0.10%	3.999	3.999	4.44	0.037
V*Qi*Qi	1	15.01	0.38%	15.011	15.011	16.67	0.000
Error	172	154.87	3.95%	154.874	0.900		
Total	191	3923.78	100.00%				

Table A.3: Accuracy of Equation 5.2

Model Summary

S	R-sq	R-sq(adj)	PRESS	R-sq(pred)	AICc	BIC
0.948911	96.05%	95.62%	193.604	95.07%	551.05	614.02

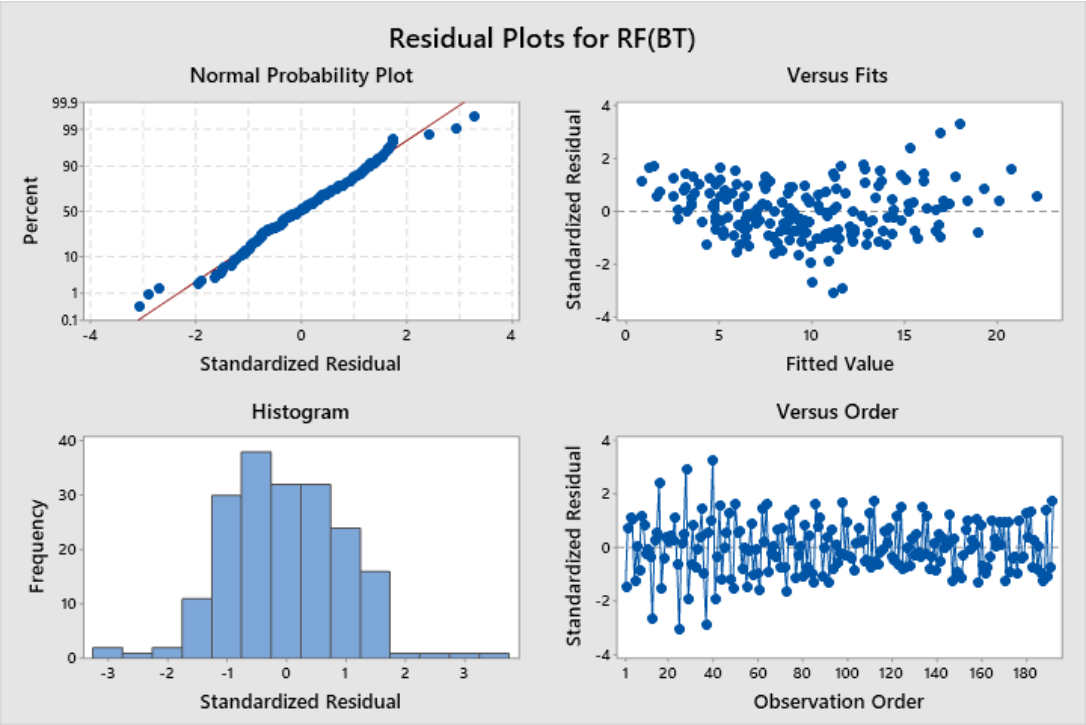

Figure A.1: Residual Plots for RF_{BT}

Results of Minitab for RF_{EOP}

Table A.4: Significance of parameters

Analysis of Variance

Source	DF	Seq SS	Contribution	Adj SS	Adj MS	F-Value	P-Value
Kz/Kx	1	685.4	6.29%	10.355	10.3545	39.19	0.000
μw	1	246.3	2.26%	18.657	18.6574	70.61	0.000
V	1	1530.9	14.05%	23.845	23.8451	90.24	0.000
Qi	1	6682.7	61.33%	62.016	62.0164	234.69	0.000
Kz/Kx*Kz/Kx	1	99.8	0.92%	11.539	11.5392	43.67	0.000
V*V	1	0.2	0.00%	17.623	17.6227	66.69	0.000
Qi*Qi	1	704.9	6.47%	26.775	26.7753	101.33	0.000
Kz/Kx*μw	1	15.7	0.14%	8.453	8.4533	31.99	0.000
Kz/Kx*V	1	72.8	0.67%	12.221	12.2206	46.25	0.000
Kz/Kx*Qi	1	205.9	1.89%	57.042	57.0419	215.87	0.000
μw*V	1	0.3	0.00%	21.216	21.2161	80.29	0.000
μw*Qi	1	0.5	0.00%	22.096	22.0959	83.62	0.000
Kz/Kx*Kz/Kx*Kz/Kx	1	5.9	0.05%	5.891	5.8910	22.29	0.000
V*V*V	1	11.9	0.11%	11.948	11.9483	45.22	0.000
Kz/Kx*Kz/Kx*V	1	12.4	0.11%	12.421	12.4214	47.01	0.000
Kz/Kx*Kz/Kx*Qi	1	3.8	0.04%	3.847	3.8472	14.56	0.000
Kz/Kx*μw*μw	1	20.7	0.19%	4.437	4.4372	16.79	0.000
Kz/Kx*V*V	1	1.7	0.02%	1.705	1.7054	6.45	0.012
Kz/Kx*V*Qi	1	387.6	3.56%	16.846	16.8457	63.75	0.000
Kz/Kx*Qi*Qi	1	21.6	0.20%	21.571	21.5708	81.63	0.000
μw*μw*Qi	1	2.5	0.02%	2.472	2.4724	9.36	0.003
μw*V*V	1	8.2	0.08%	8.196	8.1955	31.01	0.000
μw*V*Qi	1	113.8	1.04%	37.884	37.8840	143.37	0.000
μw*Qi*Qi	1	8.4	0.08%	8.428	8.4279	31.89	0.000
V*V*Qi	1	3.7	0.03%	7.837	7.8372	29.66	0.000
V*Qi*Qi	1	4.2	0.04%	4.165	4.1649	15.76	0.000
Error	165	43.6	0.40%	43.601	0.2642		
Total	191	10895.6	100.00%				

Table A.5: Accuracy of Equation 5.4

Model Summary

S	R-sq	R-sq(adj)	PRESS	R-sq(pred)	AICc	BIC
0.514049	99.60%	99.54%	58.6762	99.46%	326.21	407.46

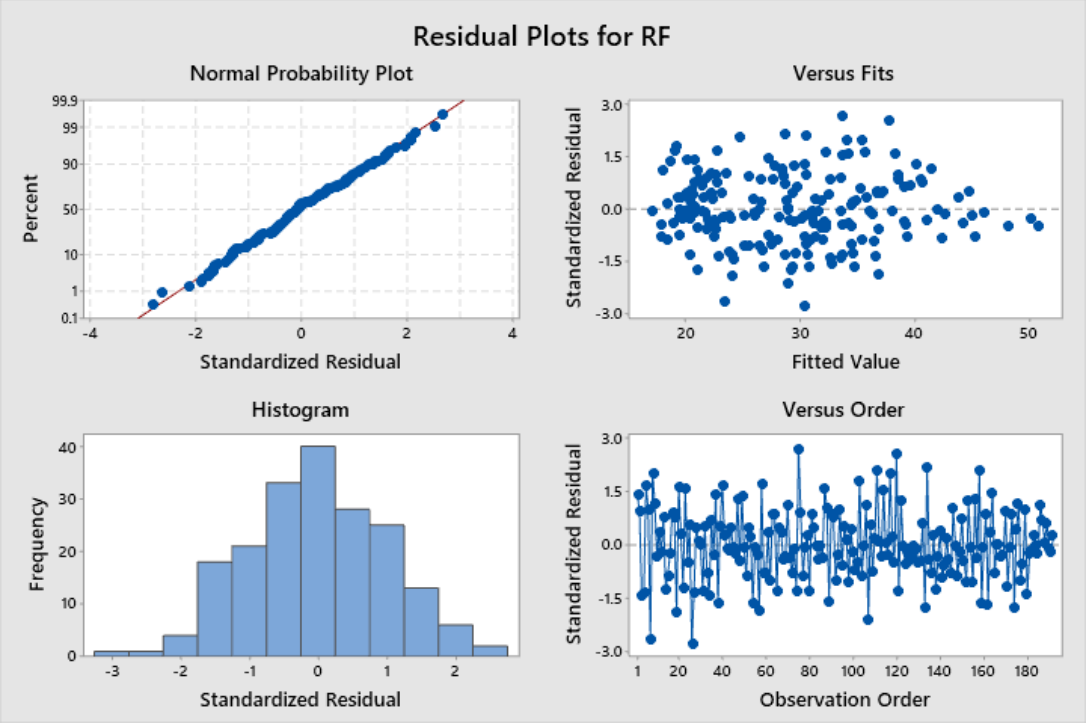

Figure A.2: Residual Plots for RF_{EOP}

Appendix B

Detailed calculations of the average absolute percent difference for all cases

Table B.1: Results of average absolute percent difference for 144 data points at BT

kz/kx	μ_w (cp)	*V*	*qi* (Mstb/d)	RF_{BT}	*Equation (5.1)*	*Error %*	*Equation (5.2)*	*Error %*
0.1	0.25	0.3	2	4.6	5.4	18.0	5.6	21.3
0.1	0.25	0.3	5	2.7	1.8	33.6	1.9	29.7
0.1	0.25	0.3	10	2.1	2.1	1.6	1.5	29.4
0.3	0.25	0.3	2	10.9	9.6	12.0	9.6	12.2
0.3	0.25	0.3	5	4.5	5.5	22.6	5.6	24.1
0.3	0.25	0.3	10	3.2	3.6	13.7	3.1	3.0
0.5	0.25	0.3	2	10.1	10.6	5.2	10.5	4.4
0.5	0.25	0.3	5	6.4	6.6	3.8	6.8	5.6
0.5	0.25	0.3	10	4	3.5	12.3	3.1	23.6
1	0.25	0.3	2	9.4	9.6	1.8	9.8	4.0
1	0.25	0.3	5	8.6	8.2	4.9	8.7	1.5
1	0.25	0.3	10	5.6	5.8	3.4	5.7	2.0
0.1	0.5	0.3	2	6.5	7.7	18.5	7.8	19.6
0.1	0.5	0.3	5	4.5	3.6	19.2	4.0	12.2
0.1	0.5	0.3	10	3.7	3.7	0.2	3.3	10.8
0.3	0.5	0.3	2	14.4	12.5	13.1	12.2	15.1
0.3	0.5	0.3	5	6.8	7.9	16.7	8.1	19.0
0.3	0.5	0.3	10	5.3	5.7	7.7	5.4	1.4
0.5	0.5	0.3	2	14.5	14.1	3.0	13.5	6.8
0.5	0.5	0.3	5	9	9.5	5.7	9.6	6.6
0.5	0.5	0.3	10	6.3	5.9	6.4	5.7	10.2
1	0.5	0.3	2	13.2	13.8	4.5	13.0	1.2
1	0.5	0.3	5	12.5	11.6	7.0	11.9	5.1
1	0.5	0.3	10	8.3	8.4	1.8	8.6	3.6
0.1	0.75	0.3	2	7.8	9.1	16.5	9.3	19.0
0.1	0.75	0.3	5	5.6	4.7	15.6	5.3	5.0
0.1	0.75	0.3	10	5	4.8	4.2	4.4	11.4
0.3	0.75	0.3	2	16.1	14.5	10.1	14.2	11.9
0.3	0.75	0.3	5	8.4	9.5	13.4	9.9	18.0
0.3	0.75	0.3	10	6.8	7.2	5.6	7.0	2.3
0.5	0.75	0.3	2	16.8	16.5	1.9	15.8	5.9
0.5	0.75	0.3	5	10.5	11.5	9.3	11.7	11.9
0.5	0.75	0.3	10	8.3	7.6	8.2	7.6	8.8
1	0.75	0.3	2	16.1	16.8	4.4	15.6	2.9
1	0.75	0.3	5	14.8	14.0	5.4	14.3	3.4

1	0.75	0.3	10	10	10.3	2.6	10.8	8.0
0.1	1	0.3	2	8.8	9.9	12.8	10.1	14.8
0.1	1	0.3	5	6.6	5.4	18.0	6.0	9.1
0.1	1	0.3	10	6	5.7	4.9	4.9	18.8
0.3	1	0.3	2	17.1	15.8	7.5	15.5	9.6
0.3	1	0.3	5	9.6	10.6	10.8	11.0	15.0
0.3	1	0.3	10	8	8.4	5.0	7.9	1.8
0.5	1	0.3	2	18.8	18.2	3.1	17.4	7.4
0.5	1	0.3	5	11.8	12.9	9.3	13.2	11.9
0.5	1	0.3	10	9.3	9.0	3.0	8.8	5.4
1	1	0.3	2	18.3	19.0	3.6	17.5	4.3
1	1	0.3	5	16.3	15.7	3.9	16.0	1.5
1	1	0.3	10	11.6	11.6	0.2	12.3	6.2
0.1	0.25	0.5	2	4.6	5.1	11.0	5.3	14.2
0.1	0.25	0.5	5	3	2.1	29.7	1.9	35.8
0.1	0.25	0.5	10	2.5	2.5	0.5	2.8	11.1
0.3	0.25	0.5	2	9.7	8.8	9.1	9.0	7.3
0.3	0.25	0.5	5	4.8	5.5	14.0	5.4	11.6
0.3	0.25	0.5	10	3.7	3.9	4.7	4.1	11.9
0.5	0.25	0.5	2	8.8	9.5	7.6	9.7	10.3
0.5	0.25	0.5	5	6.2	6.3	1.8	6.3	1.2
0.5	0.25	0.5	10	4.3	3.6	16.3	3.8	10.7
1	0.25	0.5	2	7.8	7.8	0.2	8.3	6.4
1	0.25	0.5	5	7.6	7.4	2.2	7.6	0.1
1	0.25	0.5	10	5.6	5.8	4.5	5.9	4.5
0.1	0.5	0.5	2	6.6	7.5	14.2	7.6	15.6
0.1	0.5	0.5	5	4.8	4.1	13.8	4.2	13.3
0.1	0.5	0.5	10	4.2	4.4	4.2	4.8	13.7
0.3	0.5	0.5	2	13.2	11.8	10.5	11.8	10.4
0.3	0.5	0.5	5	7.3	8.0	10.1	8.0	10.2
0.3	0.5	0.5	10	5.9	6.2	5.1	6.6	11.7
0.5	0.5	0.5	2	12.6	12.9	2.6	12.9	2.1
0.5	0.5	0.5	5	9	9.3	3.2	9.3	3.2
0.5	0.5	0.5	10	6.9	6.3	9.1	6.6	4.1
1	0.5	0.5	2	11.5	11.8	2.9	11.7	2.1
1	0.5	0.5	5	11.4	10.9	4.4	10.9	4.3
1	0.5	0.5	10	8.5	8.8	3.9	8.9	5.0
0.1	0.75	0.5	2	8.1	9.1	11.9	9.3	15.0
0.1	0.75	0.5	5	6.2	5.4	12.8	5.7	8.0
0.1	0.75	0.5	10	5.7	5.7	0.1	6.1	6.7
0.3	0.75	0.5	2	15.1	13.9	8.3	14.0	7.5
0.3	0.75	0.5	5	9	9.8	8.5	10.0	11.6

0.3	0.75	0.5	10	7.6	7.9	4.2	8.4	9.9
0.5	0.75	0.5	2	15.3	15.3	0.2	15.3	0.2
0.5	0.75	0.5	5	10.8	11.4	5.1	11.6	7.6
0.5	0.75	0.5	10	8.7	8.3	5.0	8.7	0.1
1	0.75	0.5	2	14.2	14.7	3.2	14.5	2.1
1	0.75	0.5	5	13.9	13.3	4.5	13.5	2.7
1	0.75	0.5	10	10.7	11.0	2.5	11.3	5.6
0.1	1	0.5	2	9.1	10.0	10.4	10.3	13.3
0.1	1	0.5	5	7.3	6.3	14.2	6.6	10.1
0.1	1	0.5	10	6.8	6.8	0.7	6.7	1.4
0.3	1	0.5	2	16.2	15.3	5.7	15.4	4.9
0.3	1	0.5	5	10.3	11.0	6.9	11.4	10.2
0.3	1	0.5	10	9.1	9.4	3.1	9.4	3.6
0.5	1	0.5	2	17.3	17.1	1.4	17.1	1.1
0.5	1	0.5	5	12.3	12.9	4.6	13.3	7.8
0.5	1	0.5	10	10.2	9.9	2.7	10.1	0.8
1	1	0.5	2	16.4	16.6	1.4	16.6	1.1
1	1	0.5	5	15.8	14.9	5.5	15.5	2.1
1	1	0.5	10	12.3	12.6	2.4	13.0	5.7
0.1	0.25	0.7	2	4.8	4.9	3.1	4.9	2.7
0.1	0.25	0.7	5	3.6	2.8	23.3	2.0	45.7
0.1	0.25	0.7	10	3.2	3.6	11.8	4.1	27.2
0.3	0.25	0.7	2	8.7	8.2	5.7	8.4	3.3
0.3	0.25	0.7	5	5	5.8	15.1	5.1	2.6
0.3	0.25	0.7	10	4.4	4.7	7.4	5.2	17.7
0.5	0.25	0.7	2	7.8	8.5	8.6	8.9	13.6
0.5	0.25	0.7	5	6.2	6.3	1.7	5.8	6.6
0.5	0.25	0.7	10	5.1	4.3	15.5	4.6	9.4
1	0.25	0.7	2	6.8	6.1	9.7	6.8	0.3
1	0.25	0.7	5	6.8	7.0	3.0	6.5	4.7
1	0.25	0.7	10	6.3	6.5	3.3	6.0	4.9
0.1	0.5	0.7	2	7.2	7.6	6.0	7.5	3.9
0.1	0.5	0.7	5	5.8	5.1	12.5	4.4	24.7
0.1	0.5	0.7	10	5.4	5.8	7.1	6.2	15.7
0.3	0.5	0.7	2	12.1	11.4	5.9	11.4	5.6
0.3	0.5	0.7	5	8	8.6	7.1	8.0	0.0
0.3	0.5	0.7	10	7	7.4	5.9	7.8	11.5
0.5	0.5	0.7	2	11.5	12.0	4.6	12.2	6.1
0.5	0.5	0.7	5	9.3	9.5	2.0	9.0	3.4
0.5	0.5	0.7	10	8.3	7.4	11.4	7.6	8.7
1	0.5	0.7	2	10.2	10.1	0.9	10.4	2.4
1	0.5	0.7	5	10.5	10.6	0.7	10.0	5.1

1	0.5	0.7	10	9.8	9.9	1.3	9.2	5.7
0.1	0.75	0.7	2	8.9	9.4	5.7	9.3	5.0
0.1	0.75	0.7	5	7.4	6.6	10.5	6.1	17.7
0.1	0.75	0.7	10	7.1	7.4	4.8	7.7	8.9
0.3	0.75	0.7	2	14.5	13.6	6.2	13.7	5.3
0.3	0.75	0.7	5	10	10.5	5.4	10.2	1.7
0.3	0.75	0.7	10	9.5	9.5	0.2	9.7	2.6
0.5	0.75	0.7	2	14.6	14.5	0.4	14.9	1.7
0.5	0.75	0.7	5	11.3	11.8	4.0	11.5	1.7
0.5	0.75	0.7	10	10.5	9.7	7.4	9.8	6.2
1	0.75	0.7	2	12.8	12.9	0.4	13.4	4.6
1	0.75	0.7	5	13	13.1	0.5	12.8	1.8
1	0.75	0.7	10	12.4	12.5	0.6	11.8	4.8
0.1	1	0.7	2	10.2	10.6	4.2	10.5	3.2
0.1	1	0.7	5	8.7	7.7	10.9	7.1	18.1
0.1	1	0.7	10	8.5	8.9	4.8	8.5	0.4
0.3	1	0.7	2	15.5	15.2	2.1	15.4	0.9
0.3	1	0.7	5	11.6	12.0	3.6	11.7	0.5
0.3	1	0.7	10	11.2	11.3	0.8	11.0	1.8
0.5	1	0.7	2	16.1	16.4	1.7	16.8	4.4
0.5	1	0.7	5	12.9	13.5	4.4	13.3	3.2
0.5	1	0.7	10	12.4	11.8	5.2	11.4	7.8
1	1	0.7	2	14.9	14.7	1.1	15.6	4.9
1	1	0.7	5	14.9	14.8	0.5	14.9	0.2
1	1	0.7	10	14.3	14.5	1.6	13.7	4.4
					AAPCD	6.9	AAPCD	8.3

Table B.2: Results of average absolute percent difference for 144 data at EOP

kz/kx	*μw(cP)*	*V*	*qi(Mstb/d)*	*RF*	*Equation (5.3)*	*Error %*	*Equation (5.4)*	*Error %*
0.1	0.25	0.3	2	19.3	19.0	1.7	18.9	1.9
0.1	0.25	0.3	5	26	25.7	1.1	25.7	1.1
0.1	0.25	0.3	10	30.5	30.8	1.1	30.9	1.4
0.3	0.25	0.3	2	20.4	20.5	0.3	20.4	0.2
0.3	0.25	0.3	5	29	28.3	2.5	28.3	2.5
0.3	0.25	0.3	10	34	34.3	0.9	34.4	1.0
0.5	0.25	0.3	2	20.2	20.7	2.4	20.7	2.4
0.5	0.25	0.3	5	30	29.5	1.7	29.5	1.6
0.5	0.25	0.3	10	36	36.3	0.9	36.3	0.9
1	0.25	0.3	2	19.8	19.7	0.5	19.7	0.4
1	0.25	0.3	5	31	30.7	0.9	30.7	1.0
1	0.25	0.3	10	39	39.0	0.0	38.9	0.3
0.1	0.5	0.3	2	19.5	19.7	0.9	19.6	0.3
0.1	0.5	0.3	5	27	27.5	1.7	27.4	1.4
0.1	0.5	0.3	10	33	33.0	0.1	32.9	0.2
0.3	0.5	0.3	2	21.6	21.5	0.5	21.4	1.1
0.3	0.5	0.3	5	30	30.3	1.1	30.2	0.8
0.3	0.5	0.3	10	37	36.7	0.7	36.7	0.9
0.5	0.5	0.3	2	21.7	22.0	1.5	21.9	0.9
0.5	0.5	0.3	5	32	31.9	0.4	31.8	0.8
0.5	0.5	0.3	10	39	39.0	0.1	38.9	0.2
1	0.5	0.3	2	21.6	21.8	1.0	21.7	0.3
1	0.5	0.3	5	34	33.8	0.5	33.7	1.0
1	0.5	0.3	10	42	42.4	0.9	42.2	0.5
0.1	0.75	0.3	2	19.8	19.9	0.5	20.0	0.9
0.1	0.75	0.3	5	28	28.6	2.1	28.7	2.3
0.1	0.75	0.3	10	35	34.2	2.3	34.3	2.1
0.3	0.75	0.3	2	22.3	21.9	1.9	21.9	1.6
0.3	0.75	0.3	5	31.5	31.6	0.3	31.7	0.5
0.3	0.75	0.3	10	38	38.1	0.2	38.2	0.4
0.5	0.75	0.3	2	22.5	22.6	0.4	22.6	0.5
0.5	0.75	0.3	5	33	33.3	0.9	33.3	1.0
0.5	0.75	0.3	10	41	40.5	1.2	40.6	1.0
1	0.75	0.3	2	22.5	22.8	1.2	22.8	1.2
1	0.75	0.3	5	36	35.6	1.1	35.6	1.0
1	0.75	0.3	10	44	44.2	0.4	44.2	0.5
0.1	1	0.3	2	20.2	20.1	0.5	20.2	0.1
0.1	1	0.3	5	29.3	29.5	0.7	29.6	1.0
0.1	1	0.3	10	35	35.0	0.1	35.0	0.1

0.3	1	0.3	2	22.7	22.1	2.6	22.2	2.3
0.3	1	0.3	5	32	32.5	1.7	32.6	1.8
0.3	1	0.3	10	39	38.8	0.4	38.9	0.4
0.5	1	0.3	2	23.1	22.9	1.1	22.9	1.0
0.5	1	0.3	5	34	34.2	0.7	34.3	0.8
0.5	1	0.3	10	41	41.2	0.6	41.3	0.7
1	1	0.3	2	23.1	23.1	0.1	23.0	0.4
1	1	0.3	5	36.6	36.6	0.1	36.6	0.1
1	1	0.3	10	45	44.8	0.4	44.9	0.1
0.1	0.25	0.5	2	18.5	18.4	0.7	18.4	0.4
0.1	0.25	0.5	5	24.6	25.1	2.0	25.1	2.2
0.1	0.25	0.5	10	29.5	29.5	0.1	29.6	0.4
0.3	0.25	0.5	2	19.3	19.4	0.5	19.5	1.1
0.3	0.25	0.5	5	26.9	27.1	0.7	27.2	1.1
0.3	0.25	0.5	10	32	32.3	0.9	32.4	1.2
0.5	0.25	0.5	2	20	19.3	3.5	19.5	2.7
0.5	0.25	0.5	5	27.6	27.9	1.1	28.0	1.6
0.5	0.25	0.5	10	33.6	33.7	0.3	33.8	0.6
1	0.25	0.5	2	18.5	18.2	1.7	18.5	0.2
1	0.25	0.5	5	28	28.7	2.6	28.9	3.3
1	0.25	0.5	10	35.5	35.6	0.3	35.7	0.5
0.1	0.5	0.5	2	19.1	19.4	1.4	19.3	1.1
0.1	0.5	0.5	5	26.7	26.7	0.1	26.7	0.2
0.1	0.5	0.5	10	31.5	30.9	1.9	30.8	2.2
0.3	0.5	0.5	2	20.8	20.7	0.4	20.7	0.6
0.3	0.5	0.5	5	28.9	29.0	0.5	29.0	0.3
0.3	0.5	0.5	10	34.5	33.9	1.7	33.9	1.8
0.5	0.5	0.5	2	20.8	20.9	0.6	20.9	0.6
0.5	0.5	0.5	5	30	30.1	0.5	30.1	0.4
0.5	0.5	0.5	10	36.4	35.6	2.1	35.6	2.2
1	0.5	0.5	2	20.5	20.6	0.4	20.7	0.8
1	0.5	0.5	5	31.6	31.7	0.4	31.8	0.5
1	0.5	0.5	10	39	38.2	2.0	38.2	2.0
0.1	0.75	0.5	2	19.7	20.0	1.3	20.0	1.5
0.1	0.75	0.5	5	28.4	27.8	2.2	27.8	2.1
0.1	0.75	0.5	10	31.1	31.4	1.0	31.4	0.8
0.3	0.75	0.5	2	21.5	21.5	0.2	21.5	0.1
0.3	0.75	0.5	5	30.3	30.2	0.2	30.3	0.1
0.3	0.75	0.5	10	34.3	34.6	0.8	34.5	0.7
0.5	0.75	0.5	2	21.8	21.8	0.2	21.9	0.5
0.5	0.75	0.5	5	31.6	31.5	0.3	31.6	0.1
0.5	0.75	0.5	10	36.3	36.4	0.3	36.4	0.4

1	0.75	0.5	2	21.7	21.9	0.9	22.0	1.4
1	0.75	0.5	5	33.5	33.5	0.1	33.6	0.2
1	0.75	0.5	10	39.4	39.3	0.3	39.4	0.0
0.1	1	0.5	2	20.2	20.6	1.7	20.5	1.4
0.1	1	0.5	5	29.7	28.7	3.4	28.6	3.8
0.1	1	0.5	10	31	31.5	1.5	31.2	0.8
0.3	1	0.5	2	22.1	22.1	0.0	22.0	0.4
0.3	1	0.5	5	31.4	31.2	0.7	31.1	1.1
0.3	1	0.5	10	34	34.6	1.8	34.4	1.3
0.5	1	0.5	2	22.5	22.5	0.0	22.4	0.4
0.5	1	0.5	5	32.7	32.4	0.8	32.3	1.1
0.5	1	0.5	10	36	36.5	1.3	36.3	0.9
1	1	0.5	2	22.4	22.6	0.8	22.5	0.5
1	1	0.5	5	34.7	34.4	0.9	34.4	1.0
1	1	0.5	10	39	39.3	0.7	39.3	0.8
0.1	0.25	0.7	2	17.5	17.6	0.6	17.5	0.1
0.1	0.25	0.7	5	24	23.7	1.5	23.6	1.6
0.1	0.25	0.7	10	26.5	26.4	0.4	26.4	0.3
0.3	0.25	0.7	2	18	18.2	1.3	18.2	1.0
0.3	0.25	0.7	5	25	25.2	0.6	25.1	0.5
0.3	0.25	0.7	10	29	28.5	1.8	28.5	1.8
0.5	0.25	0.7	2	17.7	17.9	1.1	17.9	0.9
0.5	0.25	0.7	5	25	25.6	2.5	25.6	2.4
0.5	0.25	0.7	10	30	29.4	2.0	29.4	2.1
1	0.25	0.7	2	17.1	16.8	1.5	16.8	1.8
1	0.25	0.7	5	26	26.3	1.1	26.2	0.8
1	0.25	0.7	10	31	30.7	1.0	30.6	1.4
0.1	0.5	0.7	2	18.7	18.7	0.2	18.7	0.2
0.1	0.5	0.7	5	25.7	25.0	2.6	25.0	2.8
0.1	0.5	0.7	10	26.1	26.8	2.7	26.8	2.6
0.3	0.5	0.7	2	19.7	19.7	0.1	19.6	0.5
0.3	0.5	0.7	5	27	26.8	0.6	26.8	0.8
0.3	0.5	0.7	10	28.5	29.2	2.3	29.1	2.2
0.5	0.5	0.7	2	19.7	19.7	0.2	19.6	0.6
0.5	0.5	0.7	5	28	27.6	1.4	27.5	1.6
0.5	0.5	0.7	10	30	30.4	1.3	30.3	1.1
1	0.5	0.7	2	19.5	19.4	0.7	19.3	1.2
1	0.5	0.7	5	29	29.0	0.0	28.9	0.4
1	0.5	0.7	10	32	32.4	1.1	32.3	0.8
0.1	0.75	0.7	2	19.6	19.5	0.6	19.6	0.1
0.1	0.75	0.7	5	26	25.8	0.6	26.0	0.1
0.1	0.75	0.7	10	26.1	26.4	1.1	26.5	1.5

0.3	0.75	0.7	2	20.7	20.6	0.4	20.7	0.0
0.3	0.75	0.7	5	28	27.8	0.7	27.9	0.3
0.3	0.75	0.7	10	28.4	28.9	1.7	29.0	2.1
0.5	0.75	0.7	2	20.9	20.7	0.7	20.8	0.4
0.5	0.75	0.7	5	29	28.7	0.9	28.8	0.6
0.5	0.75	0.7	10	30	30.2	0.8	30.4	1.2
1	0.75	0.7	2	20.8	20.8	0.2	20.9	0.4
1	0.75	0.7	5	31	30.5	1.6	30.6	1.4
1	0.75	0.7	10	32	32.5	1.7	32.6	2.0
0.1	1	0.7	2	20.3	20.3	0.1	20.4	0.4
0.1	1	0.7	5	26	26.6	2.2	26.6	2.3
0.1	1	0.7	10	26	25.6	1.6	25.6	1.6
0.3	1	0.7	2	21.4	21.5	0.3	21.5	0.3
0.3	1	0.7	5	28	28.6	2.0	28.6	2.0
0.3	1	0.7	10	29	28.1	3.2	28.1	3.2
0.5	1	0.7	2	21.7	21.6	0.4	21.6	0.5
0.5	1	0.7	5	29	29.5	1.7	29.5	1.6
0.5	1	0.7	10	30	29.4	1.9	29.4	1.9
1	1	0.7	2	21.7	21.7	0.2	21.6	0.3
1	1	0.7	5	31	31.2	0.8	31.2	0.6
1	1	0.7	10	32	31.7	1.0	31.7	0.9
					AAPCD	1.02	AAPCD	1.04

Table B.3: Results of average absolute percent difference for 48 data at BT

kz/kx	*μw(cP)*	*V*	*qi(Mstb/d)*	*RF(BT)*	*Equation (5.1)*	*Error %*	*Equation (5.2)*	*Error %*
0.1	0.25	0.1	2	6.9	5.9	14.5	5.9	14.5
0.1	0.25	0.1	5	2.4	1.8	25.0	1.9	22.2
0.1	0.25	0.1	10	1.8	2.2	23.8	0.2	89.4
0.3	0.25	0.1	2	13.9	10.5	24.4	10.2	26.9
0.3	0.25	0.1	5	5	5.9	17.6	5.8	16.3
0.3	0.25	0.1	10	2.8	4.0	43.1	2.1	26.1
0.5	0.25	0.1	2	13.6	11.9	12.4	11.4	16.3
0.5	0.25	0.1	5	8.8	7.3	17.1	7.2	17.7
0.5	0.25	0.1	10	3.8	4.0	5.5	2.3	39.9
1	0.25	0.1	2	13.9	11.5	17.3	11.3	18.8
1	0.25	0.1	5	10.7	9.2	13.7	9.9	7.6
1	0.25	0.1	10	6.9	6.3	8.4	5.6	18.8
0.1	0.5	0.1	2	7.6	8.1	6.8	7.9	4.2
0.1	0.5	0.1	5	3.8	3.6	6.4	3.7	1.5

0.1	0.5	0.1	10	3	3.7	23.8	1.8	39.0
0.3	0.5	0.1	2	17.5	13.4	23.1	12.6	27.8
0.3	0.5	0.1	5	7	8.2	17.8	8.1	16.3
0.3	0.5	0.1	10	4.5	5.9	31.4	4.2	7.5
0.5	0.5	0.1	2	17.5	15.5	11.7	14.2	18.9
0.5	0.5	0.1	5	10.6	10.1	4.3	9.9	6.6
0.5	0.5	0.1	10	5.8	6.2	7.2	4.7	18.8
1	0.5	0.1	2	17.7	16.0	9.7	14.4	18.8
1	0.5	0.1	5	14.8	12.8	13.8	12.8	13.3
1	0.5	0.1	10	9	8.7	2.8	8.3	7.6
0.1	0.75	0.1	2	8.4	9.5	12.6	9.3	10.1
0.1	0.75	0.1	5	4.8	4.6	4.9	4.9	2.8
0.1	0.75	0.1	10	4	4.7	16.8	2.8	30.4
0.3	0.75	0.1	2	19.7	15.4	21.7	14.4	26.9
0.3	0.75	0.1	5	8.2	9.8	19.4	9.8	19.3
0.3	0.75	0.1	10	5.7	7.2	26.8	5.6	2.3
0.5	0.75	0.1	2	20.1	18.0	10.6	16.3	18.9
0.5	0.75	0.1	5	11.7	12.1	3.5	11.9	1.5
0.5	0.75	0.1	10	7	7.8	10.9	6.4	8.0
1	0.75	0.1	2	20.5	19.3	6.0	16.8	18.2
1	0.75	0.1	5	17.4	15.2	12.5	15.1	13.3
1	0.75	0.1	10	10.4	10.3	0.7	10.3	0.6
0.1	1	0.1	2	9.1	10.3	12.7	9.9	8.7
0.1	1	0.1	5	5.6	5.2	7.7	5.4	3.0
0.1	1	0.1	10	4.8	5.5	13.6	3.0	36.6
0.3	1	0.1	2	21	16.8	20.0	15.5	26.2
0.3	1	0.1	5	9.2	10.9	18.1	10.7	16.7
0.3	1	0.1	10	6.7	8.3	23.8	6.3	6.2
0.5	1	0.1	2	22.2	19.8	10.8	17.7	20.2
0.5	1	0.1	5	12.6	13.5	7.4	13.2	4.4
0.5	1	0.1	10	8	9.0	12.4	7.5	6.4
1	1	0.1	2	22.7	21.7	4.3	18.5	18.6
1	1	0.1	5	18.9	17.0	10.2	16.7	11.8
1	1	0.1	10	11.3	11.4	1.1	11.7	3.3
					AAPCD	14.0	AAPCD	16.9

Table B.4: Results of average absolute percent difference for 48 data at EOP

kz/kx	*μw(cP)*	*V*	*qi(Mstb/d)*	*RF*	*Equation (5.3)*	*Error %*	*Equation (5.4)*	*Error %*
0.1	0.25	0.1	2	21.4	19.4	9.2	19.1	10.9
0.1	0.25	0.1	5	29	25.5	11.9	25.3	12.7
0.1	0.25	0.1	10	33	30.3	8.3	30.3	8.2
0.3	0.25	0.1	2	22.3	21.5	3.8	21.0	5.8
0.3	0.25	0.1	5	33	28.8	12.9	28.4	13.9
0.3	0.25	0.1	10	39	34.5	11.5	34.4	11.8
0.5	0.25	0.1	2	22.2	22.1	0.6	21.5	3.0
0.5	0.25	0.1	5	35	30.5	12.9	30.0	14.2
0.5	0.25	0.1	10	42	37.2	11.4	36.9	12.1
1	0.25	0.1	2	22.3	21.4	3.9	20.6	7.6
1	0.25	0.1	5	36	32.3	10.3	31.5	12.5
1	0.25	0.1	10	45	40.9	9.1	40.2	10.8
0.1	0.5	0.1	2	21.1	19.6	6.9	19.4	8.0
0.1	0.5	0.1	5	29	27.2	6.1	27.1	6.5
0.1	0.5	0.1	10	35	33.0	5.7	33.1	5.4
0.3	0.5	0.1	2	23.1	22.0	4.8	21.7	6.2
0.3	0.5	0.1	5	34	30.7	9.6	30.5	10.3
0.3	0.5	0.1	10	41	37.6	8.4	37.5	8.5
0.5	0.5	0.1	2	23.1	22.9	0.7	22.5	2.7
0.5	0.5	0.1	5	36.5	32.8	10.2	32.4	11.2
0.5	0.5	0.1	10	44	40.5	7.9	40.3	8.3
1	0.5	0.1	2	23.2	23.1	0.6	22.3	3.9
1	0.5	0.1	5	39	35.3	9.5	34.6	11.2
1	0.5	0.1	10	48	44.9	6.5	44.3	7.7
0.1	0.75	0.1	2	20.8	19.4	7.0	19.6	5.8
0.1	0.75	0.1	5	29	28.2	2.6	28.6	1.5
0.1	0.75	0.1	10	36	34.8	3.3	35.3	2.0
0.3	0.75	0.1	2	23.4	21.9	6.5	22.0	6.1
0.3	0.75	0.1	5	34.5	31.9	7.5	32.1	7.0
0.3	0.75	0.1	10	42	39.5	6.0	39.8	5.1
0.5	0.75	0.1	2	23.5	23.0	2.2	22.9	2.4
0.5	0.75	0.1	5	37	34.1	7.9	34.1	7.7
0.5	0.75	0.1	10	45	42.6	5.4	42.8	4.9
1	0.75	0.1	2	23.6	23.5	0.3	23.1	2.0
1	0.75	0.1	5	40	37.0	7.5	36.7	8.2
1	0.75	0.1	10	50	47.2	5.6	47.1	5.7
0.1	1	0.1	2	20.8	19.0	8.7	19.6	5.9
0.1	1	0.1	5	30	29.0	3.4	29.6	1.3
0.1	1	0.1	10	37.5	36.1	3.8	36.8	1.9

0.3	1	0.1	2	23.6	21.5	8.7	22.0	7.0
0.3	1	0.1	5	35	32.7	6.6	33.2	5.3
0.3	1	0.1	10	42.6	40.8	4.3	41.4	2.9
0.5	1	0.1	2	23.7	22.7	4.3	22.9	3.3
0.5	1	0.1	5	37.4	34.9	6.8	35.2	5.9
0.5	1	0.1	10	46	43.8	4.8	44.3	3.6
1	1	0.1	2	23.8	23.3	2.3	23.1	2.9
1	1	0.1	5	40.7	37.8	7.2	37.8	7.2
1	1	0.1	10	50.6	48.4	4.4	48.7	3.8
					AAPCD	6.5	AAPCD	6.7